LITHIUM DENTRITE GROWTH SUPPRESSION AND IONIC CONDUCTIVITY OF Li_2S-P_2S_5-P_2O_5 GLASS SOLID ELECTROLYTES PREPARED BY MECHANICAL MILLING

by

Mazlum Cengiz

B.A., Nigde Omer Halisdemir University, 2012

A thesis submitted to the

Faculty of the Graduate School of the

University of Colorado in partial fulfillment

of the requirement for the degree of

Master of Science

Department of Mechanical Engineering 2018

This thesis entitled:

LITHIUM DENTRITE GROWTH SUPPRESSION AND IONIC CONDUCTIVITY OF Li_2S-P_2S_5-P_2O_5 GLASS SOLID ELECTROLYTES PREPARED BY MECHANICAL MILLING

written by Mazlum Cengiz

has been approved for the Department of Mechanical Engineering

_____

Prof. Sehee Lee

_____

Prof. Conrad Stoldt

_____

Prof. Yifu Ding

Date_____

The final copy of this thesis has been examined by the signatories, and we find that both the content and the form meet acceptable presentation standards of scholarly work in the above mentioned discipline.

Cengiz, Mazlum (MS., Mechanical Engineering)

LITHIUM DENTRITE GROWTH SUPPRESSION AND IONIC CONDUCTIVITY OF Li_2S-P_2S_5-P_2O_5 GLASS SOLID ELECTROLYTES PREPARED BY MECHANICAL MILLING

Thesis directed by Prof. Sehee Lee

Conductivity of the $77.5Li_2S \cdot 22.5P_2S_5$ (mol %) and $77.5Li_2S.(22.5 - x).P_2S_5.xP_2O_5$ (mol %) glassy solid state electrolytes (SSEs) and possible correlation among the conductivity, density properties, varying P_2O_5 substitutions, and lithium deposition in symmetric lithium metal batteries were examined. The mechanical milling method was used to prepare the glassy SSEs. The conductivity and density of the $77.5Li_2S.22.5P_2S_5$ (mol %) glassy electrolyte could be enhanced by adding a small amount of P_2O_5. The Li/$77.5Li_2S.(22.5–x).P_2S_5.xP_2O_5$ (mol %)/Li metal cells with P_2O_5 substitution of $x<9$ displayed longer cycling performance compared to Li/$77.5Li_2S \cdot 22.5P_2S_5$ (mol %)/Li metal cells. Hence, in the case of this study, the conductivity, density, and small P_2O_5 addition in the $77.5Li_2S \cdot 22.5P_2S_5$ (mol %) glassy electrolyte would be the main factors of reduced dendrite growth.

Dedication

This thesis is dedicated to family.

To my parents, Abdurrahman and Fatma, who have always supported and trusted me.

To my sister, Xhezal for being a great role model.

To my brother, Selami for being my spiritual guide.

To my girlfriend, Richa who has made my life more meaningful.

Acknowledgements

Prof. Sehee Lee: A great mentor, adviser and role model who gave me an opportunity to study in his electrochemical energy lab and a chance to acquire research experience. His work ethic and professionalism has truly impacted my life and has made me feel passionate about pursuing my career in the field of electrochemistry.

The Electrochemical Energy Laboratory: My co-workers, my friends, Hyukkeun Oh, Ashley Heist, Nathan Dunlap, and Simon Elnicki Hafner, were always helpful and kind.

Contents

Figures

1. Introduction

As rechargeable power sources, lithium ion batteries (LIBs) have attracted remarkable attention because they offer high energy density, flexible and lightweight design, good shelf life, no memory effects and long lifetime[1-3]. LIBs are essential technologies because of their demanding applications, such as portable electronics, electric vehicles, and grid energy storage. For the safety concerns regarding flammability and toxicity, utilizing the conventional liquid electrolyte system for LIBs has many limitation[3-4]. Therefore, replacing organic liquid electrolytes with solid-state electrolytes (SSEs) has great potential to improve the safety properties of next-generation LIBs because of the possible advantages such as high electrochemical, and thermal stability of SSEs[1,5-10]. Moreover, the solid-state electrolytes are less prone to issues such as electrolyte leaking and pollution unlike organic liquid electrolytes[5,6]. Among various ceramic and polymeric SSE materials, the sulfide electrolytes, such as $Li_{10}MP_2S_{12}$ crystals, Li_2S-SiS_2, and Li_2S-P_2S_5 glass ceramics, have lithium-ion conductivities of 10^{-4} S cm^{-1} or even as high as an order of 10^{-3} S cm^{-1} at room temperature[5,21,22]. Also, sulfide based glass-ceramic electrolytes are chemically stable at high temperatures and can be easily processed by cold-compacting the powder[24,25]. This allows the SSEs to be formed into a thin layer with a large area to obtain a low internal resistance and thus provide a high current produced from the battery[5]. Additionally, in order to form a tri-layer pellet, high pressure can be applied to the powder forms of cathode, electrolyte, and anode during the assembly of bulk solid-state cells[23].

Another important advantage that has been predicted of SSEs was the ability to suppress lithium metal dendrite growth[9,25]. Energy density of the battery system can be improved significantly with lithium metal anodes which have high mass specific capacity (3869 mAh/g) and

low density (0.534 g/cm3)[2]. However, the growth of lithium dendrites and the subsequent short circuiting phenomenon leading to safety hazards, such as thermal runaway and combustion has been a critical roadblock to the widespread application of lithium metal anode systems[2].

However, uncontrolled dendritic and mossy lithium growth is still a challenge for solid state batteries and the mechanism is not well understood[14,26,27,28-33]. There is no confirmed model showing the exact mechanism of dendrite growth through SSEs[14,26,27,28-33]. Lithium creates heterogeneous depositions during charging of the cells, which causes the growth of lithium dendrites[23,26,34]. Presenting a buffer layer between the lithium metal and electrolyte, varying electrolyte composition, density or the lithium microstructure, and using self-healing polymers as composite fillers are some of the methods published in literature for improvement of the electrode-electrolyte interface[23,26,34]. Recently, Porz, L. et al. reported that SSE surface morphology, specifically defect size such as surface cracks, and defect density are important factors for the onset of uncontrolled dendritic lithium growth[35]. Li-planting in pre-existing flaws creates crack-tip stresses which accelerate crack propagation[35].

Tao, Y. et al. reported a glass-ceramic electrolyte based on Li_2S-P_2S_5-P_2O_5 with high ionic conductivity and chemical stability against lithium metal[34]. The composition of $75Li_2S.24P_2S_5.1P_2O_5$ was determined to be optimal with the highest conductivity and lowest activation energy among various P_2O_5 compositions and showed stable cycling of Li metal cells without short circuiting[34]. The addition of small amounts of oxygen to sulfide-based materials had been shown to improve the conductivity and chemical stability previously[36-42].

The Young's modulus was measured[43].

The present study reports conductivity properties of the Li_2S-P_2S_5 and Li_2S-P_2S_5-P_2O_5 glassy electrolytes and the possible correlation between the properties of the electrolytes and

lithium metal deposition. The results declare an examination of the glassy electrolytes in the range of $77.5Li_2S\cdot(22.5 - x)P_2S_5\cdot xP_2O_5$ (mol %) for x=0, 0.25, 0.5, 1, 2, 3, 6, 9.

2. Experimental

The mechanical milling technique was used for preparation of the $77.5Li_2S.22.5P_2S_5$ and $77.5Li_2S\cdot(22.5 - x)P_2S_5\cdot xP_2O_5$ (mol %) glassy electrolytes. As starting materials, Li_2S (Alfa Aesar 99.9%), P_2S_5 (Sigma-Alderich, 99%), and P_2O_5 (Alfa Aesar 99.9%) crystalline powders were utilized to prepare the glassy SSEs. Proper composition of the starting materials were combined into a stainless ball jar with 3 large stainless steel balls (10mm diameter), and 20 small stainless steel balls (6mm diameter). High energy ball milling was carried out for 20 hours by a planetary ball mill apparatus (SFM-1 Desk-Top Planetary Ball Miller) and rotating speed was 400 rpm. The mass measurements and preparation of the mixture was conducted at 24 C° in a dry Argon-filled glove box. Symmetric lithium metal cells were created to reveal dendrite initiation and growth in the $77.5Li_2S\cdot(22.5 - x)P_2S_5\cdot xP_2O_5$ (mol %) glasses. Electrolyte pellets were formed by cold pressing under 75 MPa in a polyetheretherketone (PEEK)-lined titanium die for 3 minutes and then the pressure was increased to 375 MPa tons and pressed for 5 minutes. Ionic conductivities were measured by AC impedance spectroscopy with a Solarton 1280C with a frequency from 20 kHz to 0.01 Hz at 60 °C. Thickness of the pellets were range of 0.06096-0.08128 cm which equated to approximately a 0.113 g cm^{-2} mass loading. Figure 1a represents an image of a prepared pellet. For both galvanostatic and polarization experiments, the cell construction was Li foil/$77.5Li_2S\cdot(22.5 - x)P_2S_5\cdot xP_2O_5$ (mol %) /Li foil. Li metal foil with 0.75 mm thickness (Alfa-Aesar) was attached to the $77.5Li_2S\cdot(22.5 - x)P_2S_5\cdot xP_2O_5$ (mol %) SSE. The cell was pressed by

using a torque wrench at 20 inch pound (corresponding to approximately 20 MPa) for both galvanostatic and polarization tests. Galvanostatic charge and discharge cycling and polarization tests occurred at a current density of 0.1 mA/cm^{-2}. Schematic diagram for symmetric Li metal cells with the $77.5Li_2S{\cdot}22.5P_2S_5$ and $77.5Li_2S{\cdot}(22.5 - x)P_2S_5{\cdot}xP_2O_5$ (mol %) SSEs are illustrated in figure 1b and 1c, respectively. Battery operation was conducted with the cell in an oven at 60 °C temperature under Argon. The rest time (the time before cycling was started) was 6 hours for the cell temperature to rise and equilibrate in the oven and cycling took an hour for each charge or discharge cycle. For polarization tests, cells were subjected to a single direction constant current until a sharp drop in voltage was observed which indicates a short circuiting event.

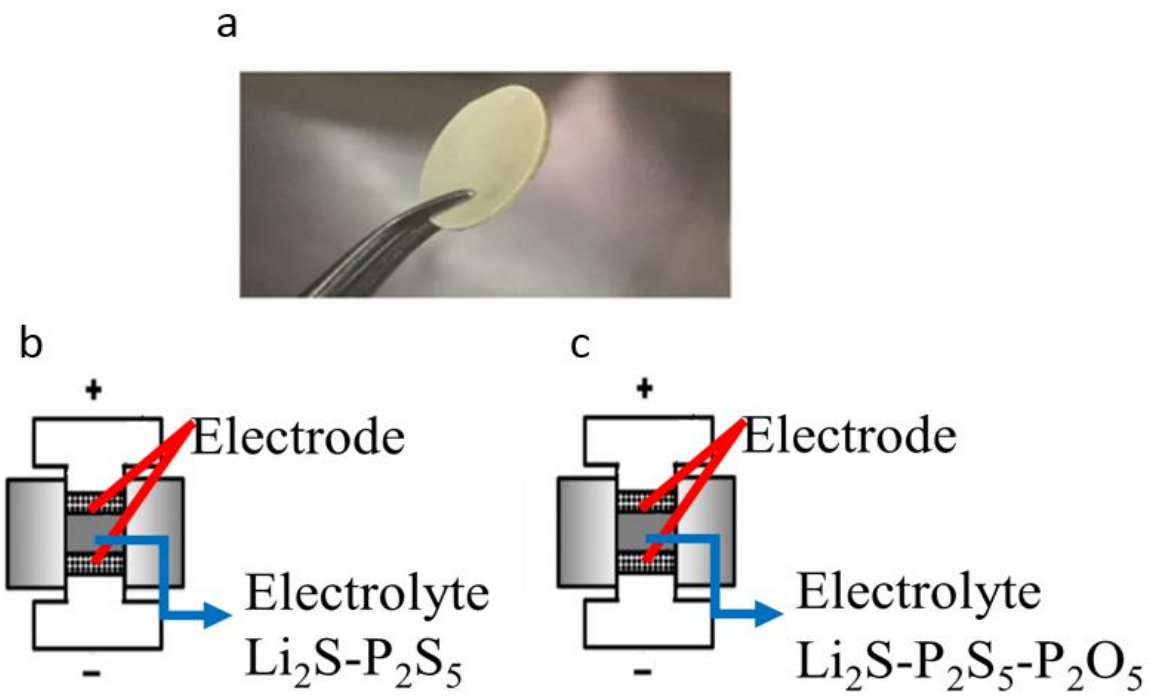

Figure 1. a) The picture of free-standing pellet. b) Schematic diagram of Li/Li lithium metal cells with the $77.5Li_2S.22.5P_2S_5$ (mol %) glasses[3]. c) Schematic diagram of Li/Li cells with the $77.5Li_2S.(22.5 - x).P_2S_5.xP_2O_5$ glasses[3].

3. Results and discussion

The $77.5Li_2S$-$22.5P_2S_5$ (mol %) glassy electrolyte shows a conductivity of 4.92 x 10^{-4} S cm^{-1} (J. M. Whiteley et al[7]) and the symmetric lithium metal cell using this electrolyte showed a good cyclability of over 30 cycles without short circuiting. Figure 2a and 2b demonstrate the cycling performance of the Li/$77.5Li_2S$-$22.5P_2S_5$ (mol %)/Li cells. The short circuit capacity of the $77.5Li_2S$-$22.5P_2S_5$ (mol %) glassy electrolyte is 3.2 mAh/cm^2. Also, the results of the deposition tests with the $77.5Li_2S$-$22.5P_2S_5$ (mol %) glassy electrolyte are displayed in figure 3.

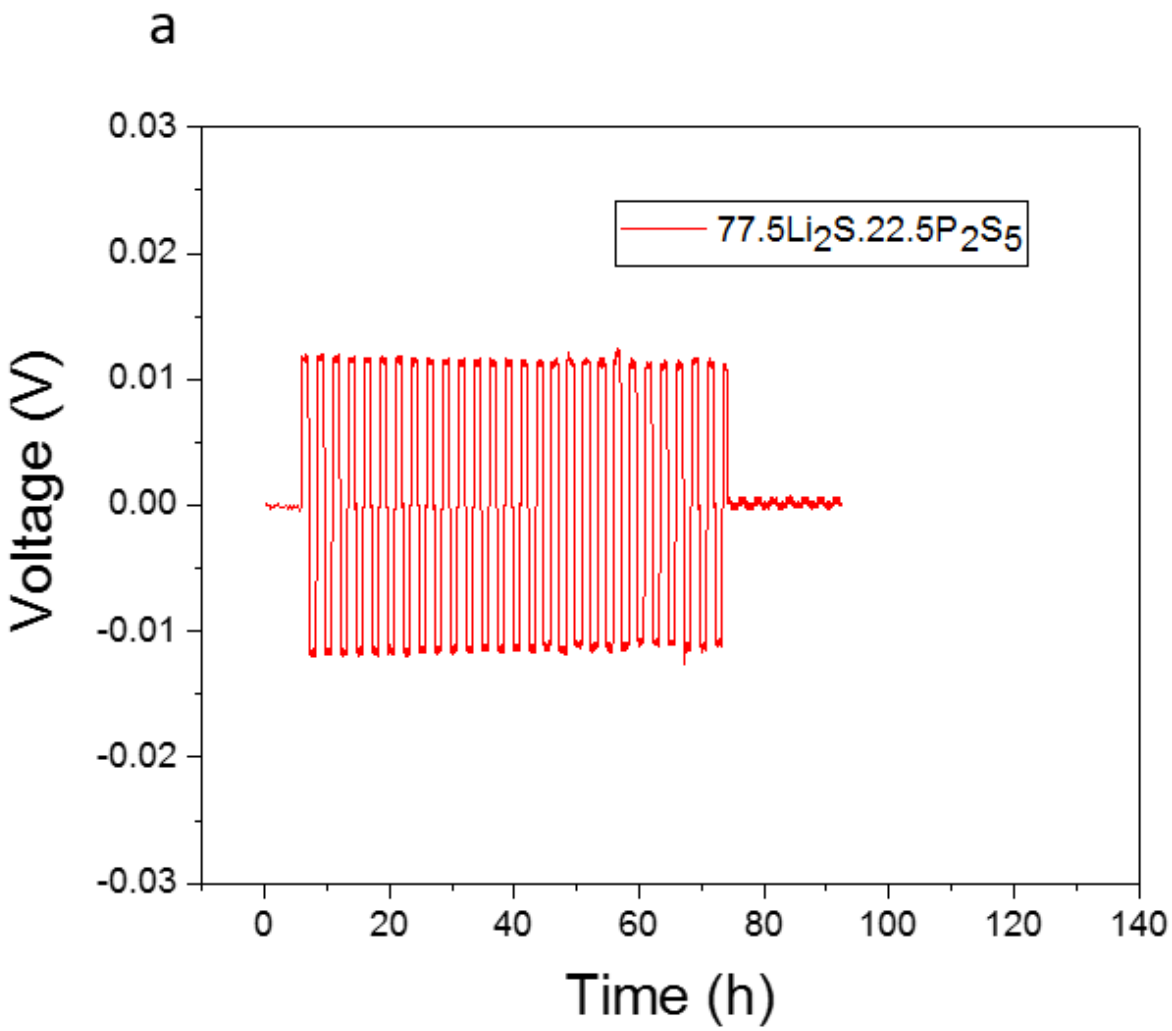

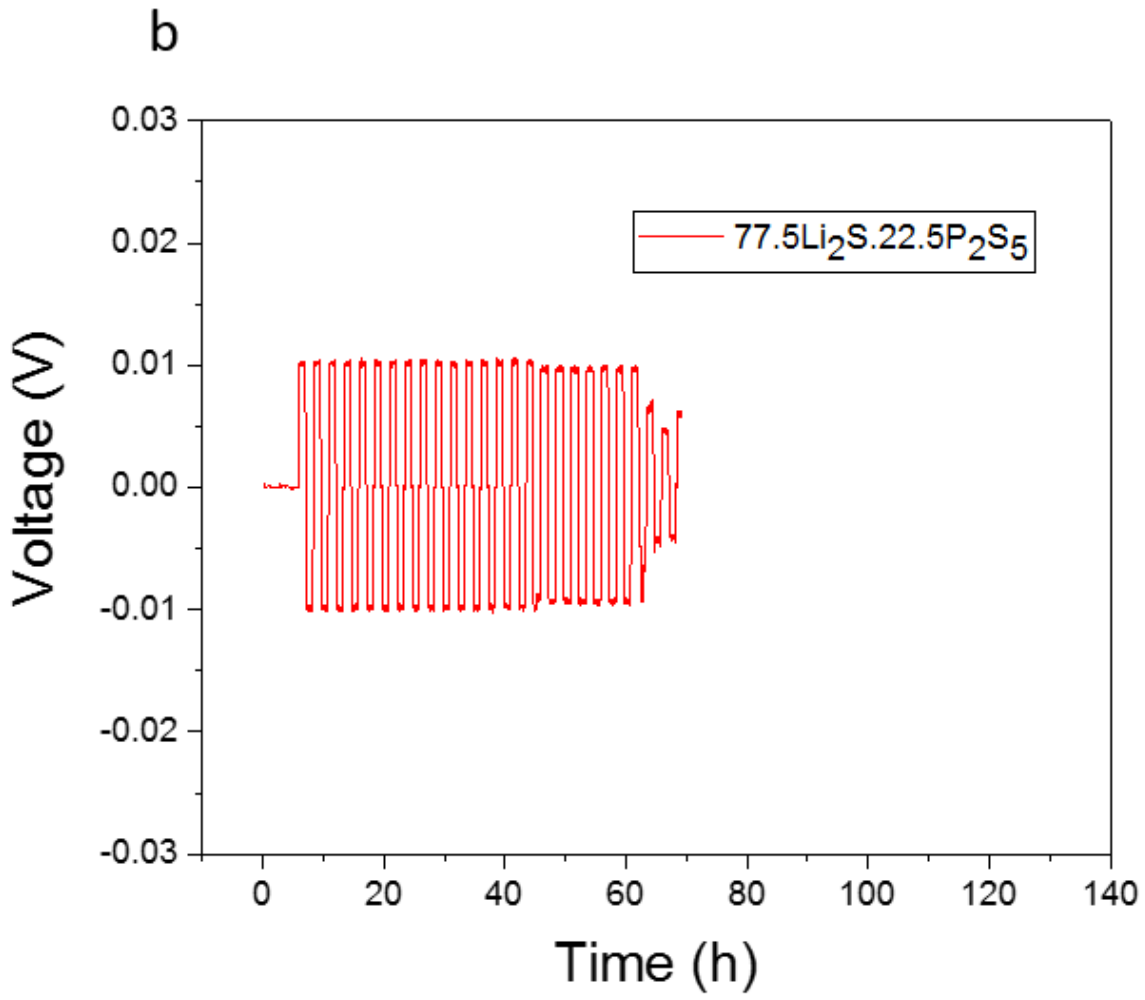

Figure 2. a) and b) show the cycling performance of the Li/77.5Li_2S.22.5P_2S_5 (mol %) /Li metal cells.

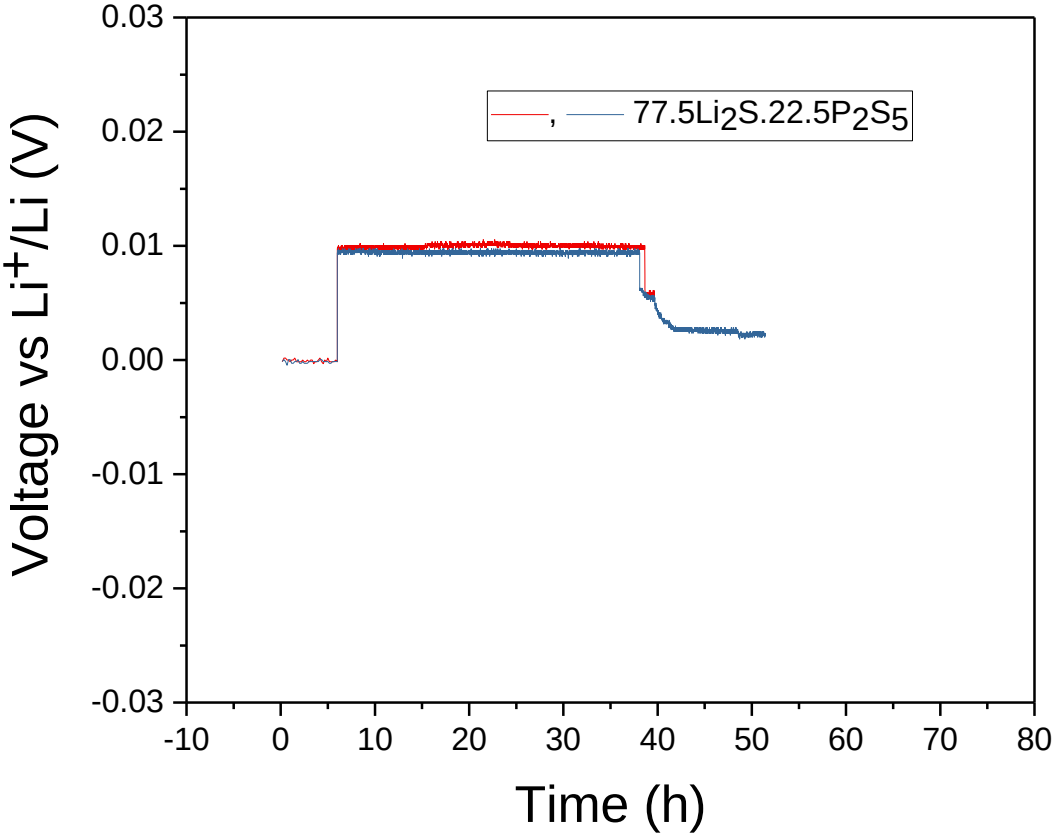

Figure 3. Galvanostatic plating of lithium metal cells with using the $77.5Li_2S.22.5P_2S_5$ (mol %) SSE.

Figure 4 demonstrates a comparison of the conductivity of the $77.5Li_2S.(22.5–x)$ $P_2S_5.xP_2O_5$ (mol %) glassy electrolytes. Also, impedance data of the Li/$77.5Li_2S.22.5.P_2S_5$ (mol %) /Li and Li/$77.5Li_2S_5$. (22.5-x) $P_2S_5.xP_2O_5$ (mol %)/Li metal cells are illustrated in figure 5a and 5b. An increasing conductivity can be seen from adding a small amount of P_2O_5. The $77.5Li_2S.$ (22.5–x) $P_2S_5.xP_2O_5$ (mol %) SSE with 0.25 mol% P_2O_5 substitution displays the highest conductivity of 6.5×10^{-4} S cm^{-1}. Tao, Y. et al. indicates that a reduction of the activation energy of Li diffusion happens when a non-bridging sulfur atom is substituted with a bridging oxygen atom[34]. This formation works as a weaker trap for Li ions[34]. Therefore, a conductivity increase in

the glassy electrolyte occurs[34]. In the case of this study, 0.25 P_2O_5 substitution could create the bridging oxygen atoms so the conductivity would be increased. However, further P_2O_5 substitution decreases the conductivity. For instance, the conductivity of 0.5 mol P_2O_5 % substitution is 5.74 $x10^{-4}$ Scm^{-1}. Moreover, the conductivity of the 77.5Li2S. $(22.5 - x)P_2S_5$ .xP_2O_5 (mol %) solid state electrolyte with 1, 2, 3, 6 and 9 mol% P_2O_5 substitution are smaller than the conductivity of the pure 77.5Li_2S. 22.5P_2S_5 (mol %) glassy electrolyte. A large P_2O_5 substitution causes of formation of the $P_2S_6^{4-}$ions with P-P bond and the PO_4^{3-} ions with non-bridging oxygen[34,39]. These formations create a stronger trap for Li diffusion so the conductivity of the electrolyte decreases[34]. In the case of this study, 1 mol % and more P_2O_5 substitution could create $P_2S_6^{4-}$ and PO_4^{3-} ions. Thus, the conductivity of glassy SSEs would be decreased by the formation of these ions.

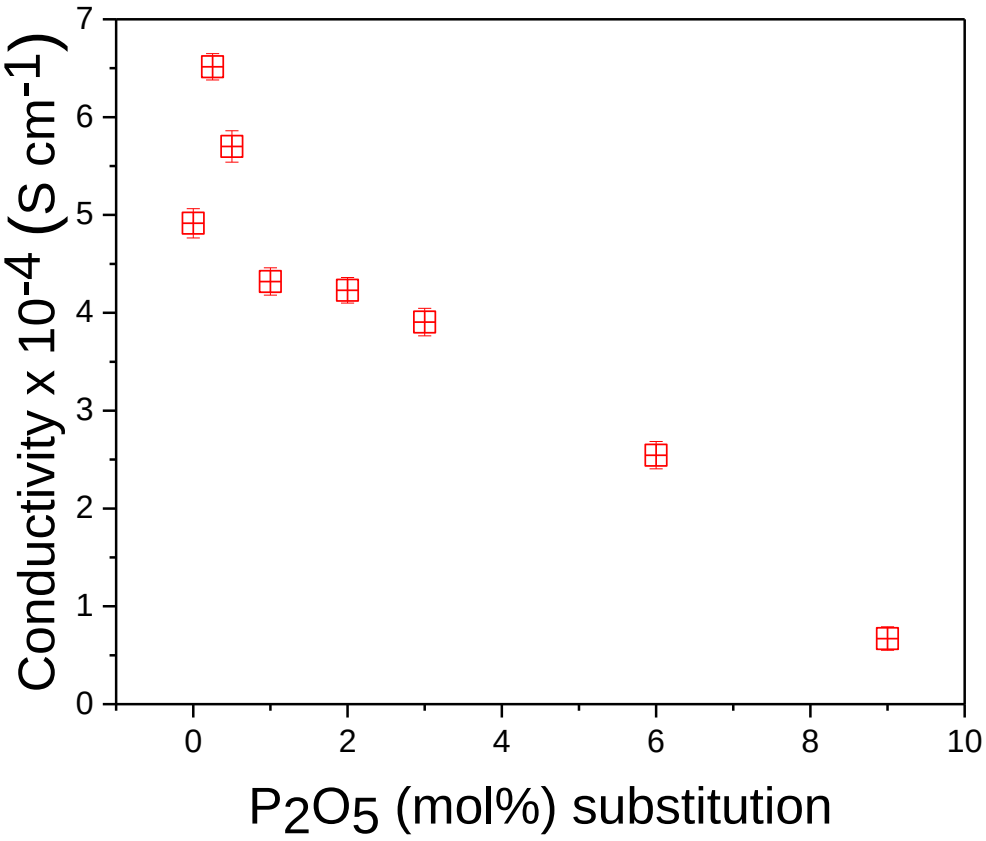

Figure 4. Composition dependence on conductivities at 60°C temperature for the Li/77.5Li_2S.(22.5 x)P_2S_5.xP_2O_5/Li metal cells.

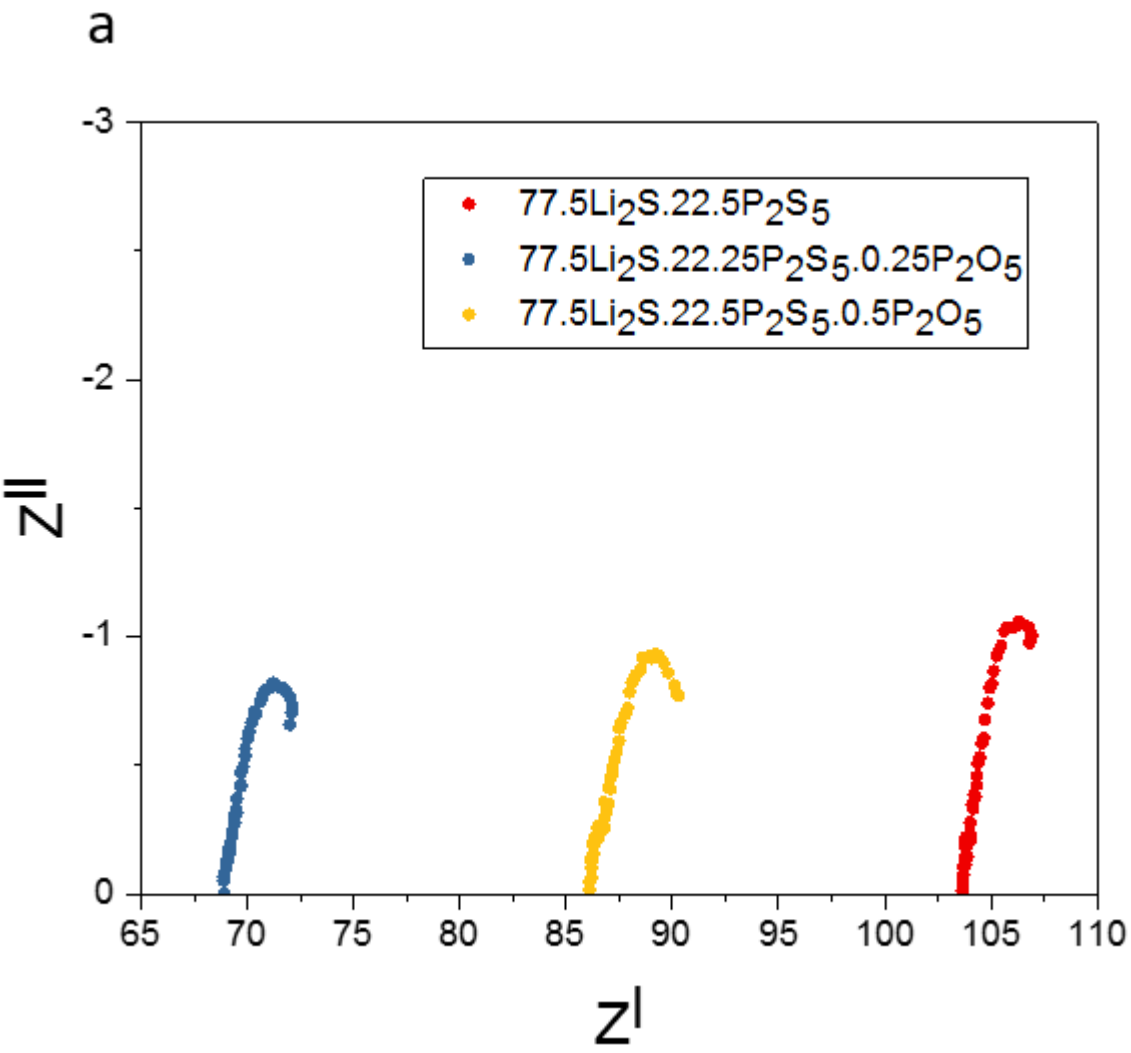
a
77.5Li2S.22.5P2S5
77.5Li2S.22.25P2S5.0.25P2O5
77.5Li2S.22.5P2S5.0.5P2O5
-3
-2
-1
0
65
70
75
80
85
90
95
100
105
110
ZII
ZI

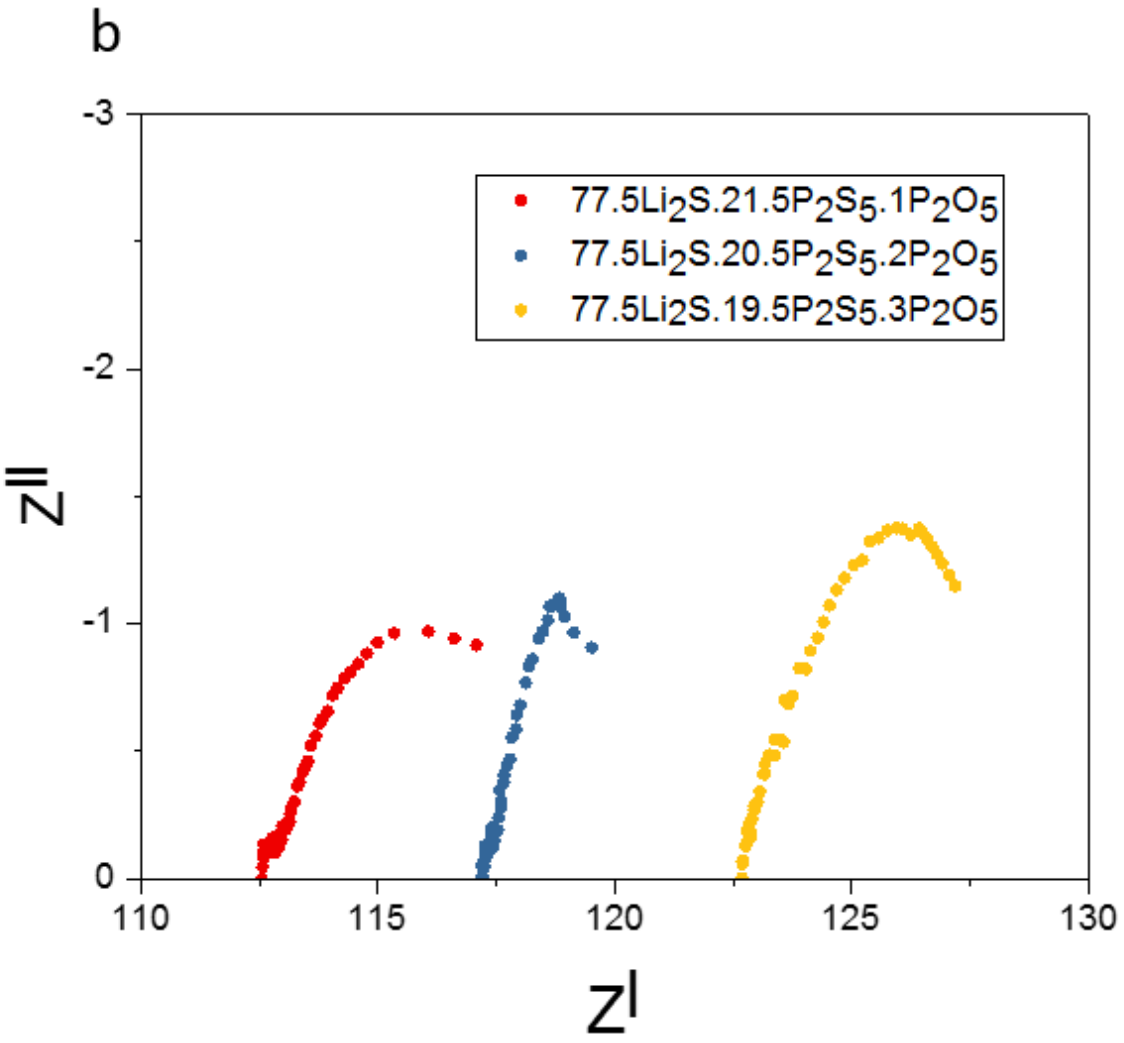

Figure 5. a) Impedance for Li/77.5Li_2S.22.5P_2S_5/Li, Li/77.5Li_2S_5.(22.25)P_2S_5.0.25P_2O_5/Li, and Li/77.5Li_2S_5.(22)P_2S_5.0.5P_2O_5/Li cells. b) Impedance for Li/77.5Li_2S_5.(21.5)P_2S_5.1P_2O_5/Li, Li/77.5Li_2S_5.(20.5)P_2S_5.2P_2O_5/Li, and Li/77.5Li_2S_5.(19.5)P_2S_5.3P_2O_5/Li cells.

Figure 6 demonstrates a correlation between composition of P_2O_5 and density of the 77.5Li_2S-22.5P_2S_5, and 77.5Li_2S_5.(22.5-x)P_2S_5.xP_2O_5 glassy electrolytes. The 77.5Li_2S.(22.5-x).P_2S_5.xP_2O_5 (mol %) glassy electrolyte with P_2O_5 substitution of x=0.25 was better compressed into a thin layer than 77.5Li_2S-22.5P_2S_5 glassy electrolyte. The increase in density might be due to change in mechanical properties of the glassy electrolyte. However, thickness of the pellets were

increased by further P_2O_5 substitution (>0.25 mol %). Moreover, the thickness of pure $77.5Li_2S{\cdot}22.5P_2S_5$ (mol %) glassy electrolyte pellet was higher than thickness of $77.5Li_2S.(22.5 - x).P_2S_5.xP_2O_5$ (mol %) with P_2O_5 substitution of x<6 pellets. Thus, a small P_2O_5 addition allows the glassy electrolyte to be better compressed into a thin layer. Kato, A. et al. reported that P_2O_5 substitution will increase the bond dissociation energy because the P-O bonds are stronger than the P-S bonds[43]. Therefore, the density will increase by P_2O_5 substitution[43]. In the case of this study, 6 mol % and more P_2O_5 substitution could increase the bond dissociation energy and decrease the thickness of the pellets.

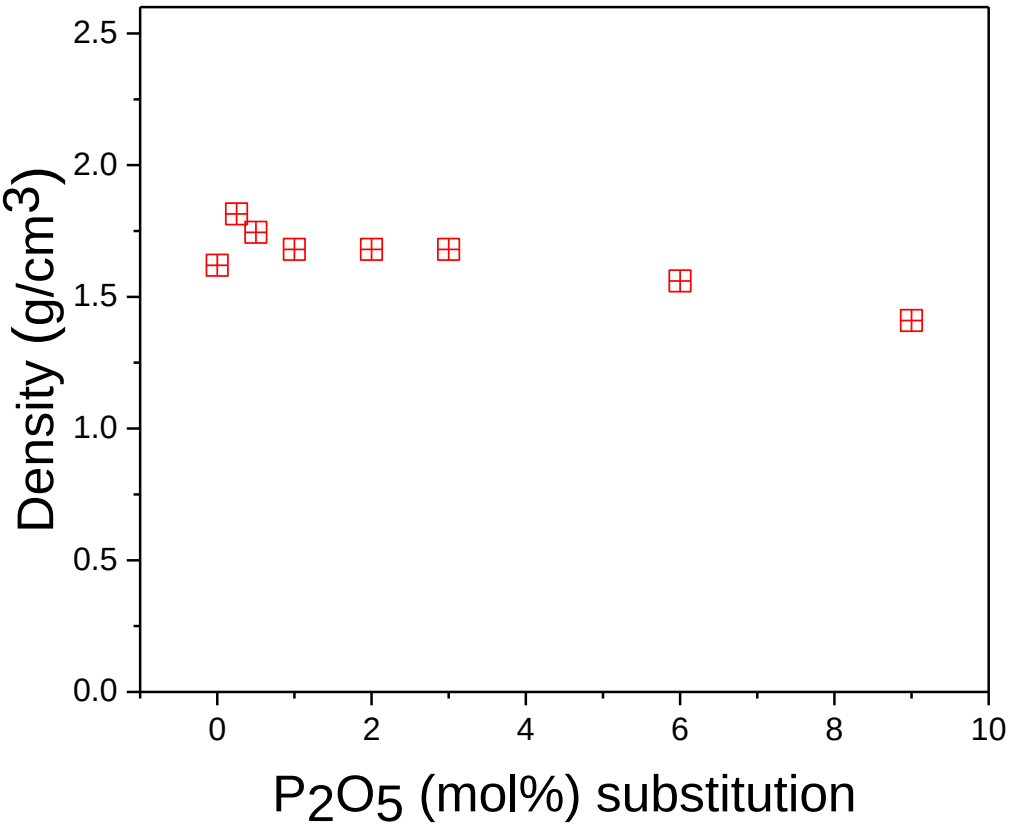

Figure 6. Density of the $77.5Li_2S.22.5P_2S_5$ (mol %) SSE, and $77.5Li_2S_5.(22.5\text{-}x)P_2S_5.xP_2O_5$ (mol%) glassy electrolyte with varying composition of P_2O_5.

Introducing oxide species into a sulfide based electrolyte increased the cycle stability. Figure 7 shows a comparison of the cycling numbers of Li/Li metal cells with the $77.5Li_2S.22.5P_2S_5$ (mol %) glassy SSE, and $77.5Li_2S.(22.5–x)P_2S_5.xP_2O_5$ (mol %) glassy electrolytes having varying substitution of P_2O_5.

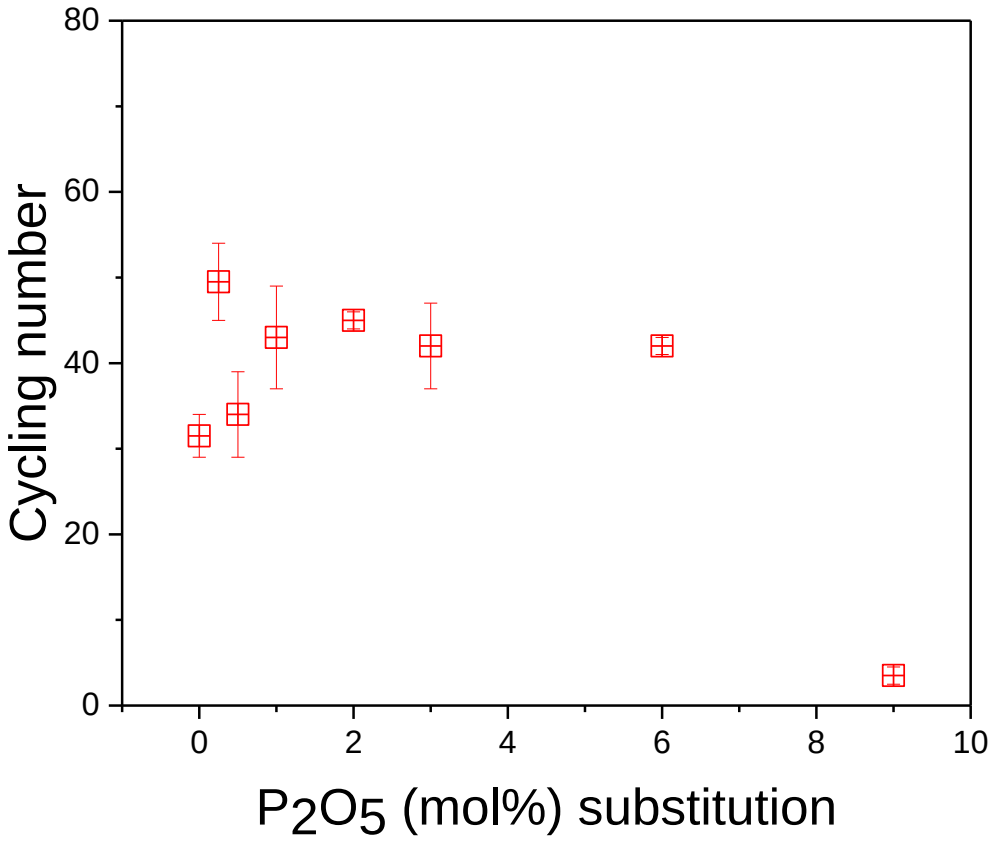

Figure 7. The cycling numbers of Li/$77.5Li_2S.(22.5\text{-}x)P_2S_5.xP_2O_5$/Li cells with varying composition of P_2O_5.

As it can be seen from cycling performance of Li/$77.5Li_2S.(22.5 – x)P_2S_5.xP_2O_5$ (mol %) /Li cells, the growth of lithium dendrites could be suppressed by adding a small amount of P_2O_5. While the cycling number of a symmetric lithium metal cell with $77.5Li_2S.22.5P_2S_5$ (mol %) glassy electrolyte is 34, the cycling number of Li/$77.5Li_2S.(22.5 – x)\ P_2S_5.xP_2O_5$ (mol %) /Li cells having

0.25% content of P_2O_5 is 54. This could be from enhanced conductivity in the electrolyte, and increased density of the pellet. However, further substitution of P_2O_5 could increase the dendrite growth effects of the Li/77.5Li_2S.(22.5 – x).xP_2O_5 (mol %)/Li metal cells since the conductivity was decreased by further P_2O_5 addition. The cycling numbers 0.5, 1, 2, 3, 6, and 9 mol % P_2O_5 are 39, 49, 46, 47, 43, and 4, respectively. Thus, Li/77.5Li_2S.(22.5 – x).P_2S_5.xP_2O_5 (mol %)/Li cells with P_2O_5 substitution of x<9 displayed longer cycling performance without short circuiting compared to cells with pure 77.5Li_2S·22.5P_2S_5 (mol %) glassy SSE. The cycling performances of Li/77.5Li_2S.(22.5 – x)P_2S_5.xP_2O_5 (mol %)/Li cells with varying composition of P_2O_5 are illustrated in figures 8a, and b (0.25 mol % P_2O_5), 9a and b (0.5 mol % P_2O_5), 10a and b (1 mol % P_2O_5), 11a and b (2 mol % P_2O_5), 12a and b (3 mol % P_2O_5), 13a and b (6 mol % P_2O_5), and 14a and b (9 mol % P_2O_5) in the next pages. Two cycling performance of each composition were displayed to support the accuracy of figure 7. Some of the figures have voltage increases in specific cycles due to temperature change in the oven.

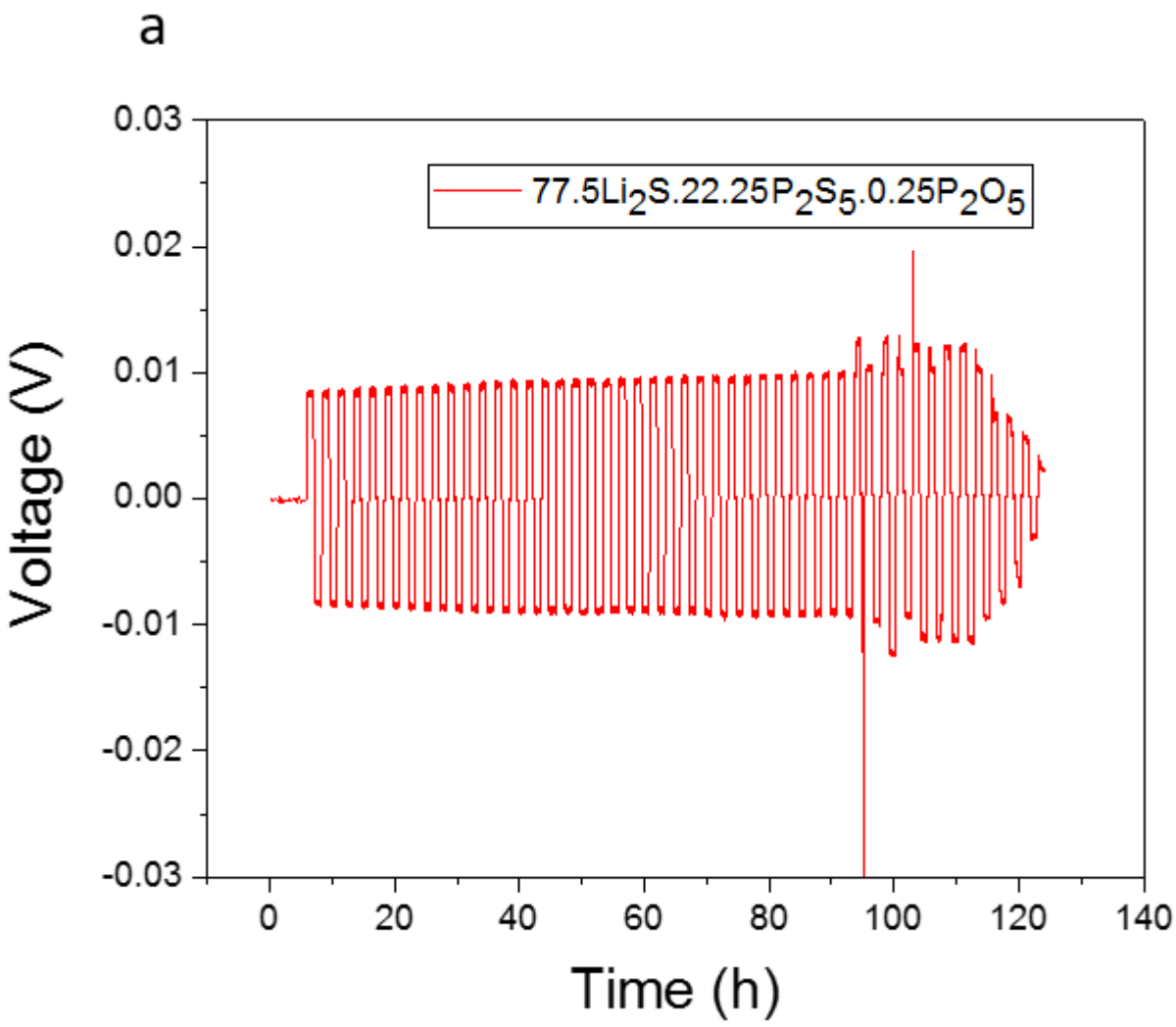
a
77.5Li2S.22.25P2S5.0.25P2O5
Voltage (V)
0.03
0.02
0.01
0.00
-0.01
-0.02
-0.03
0
20
40
60
80
100
120
140
Time (h)

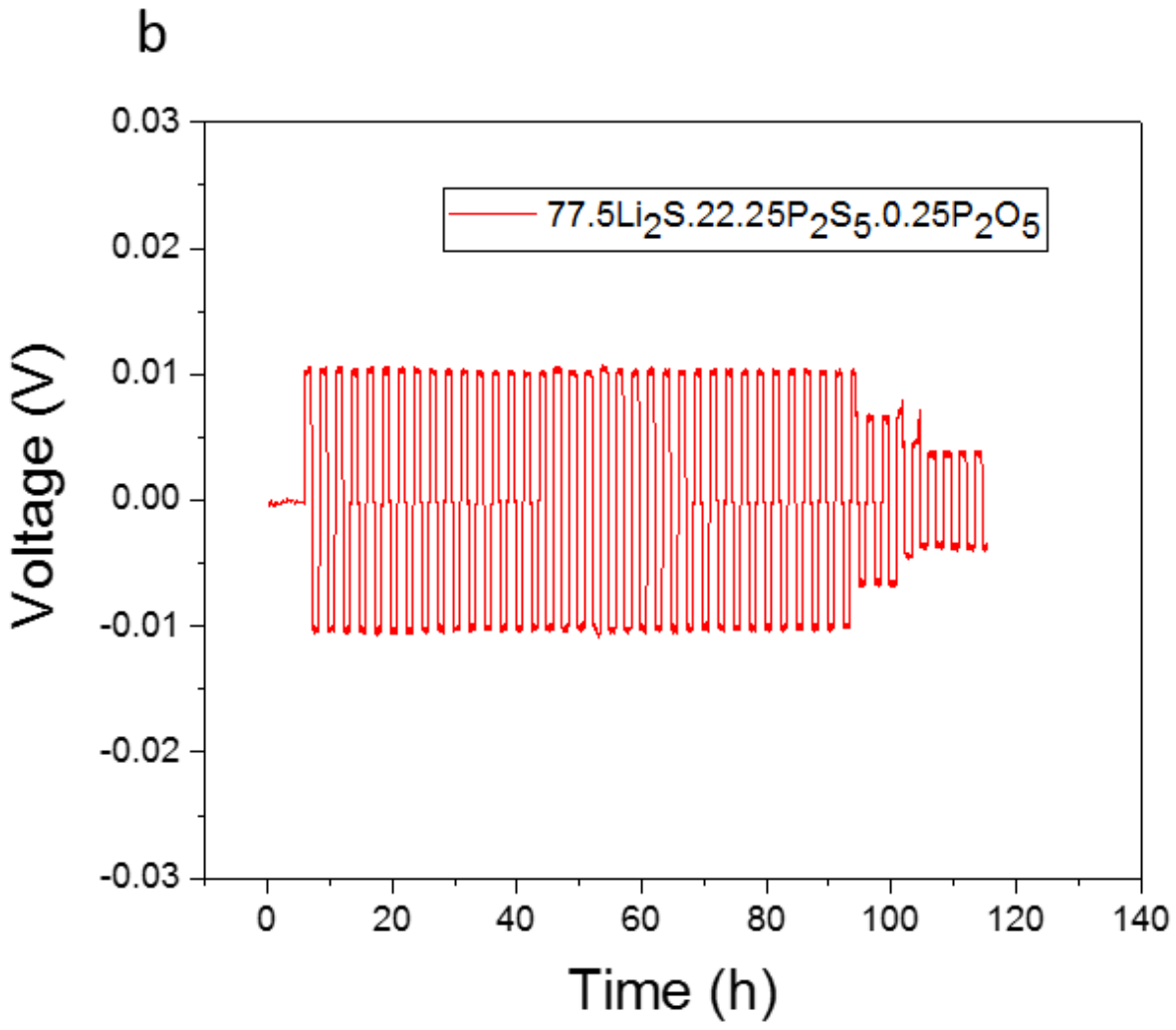

Figure 8. a) and b) show the cycling performance of the Li/77.5Li_2S.22.25P_2S_5.0.25P_2O_5 (mol %)/Li metal cells.

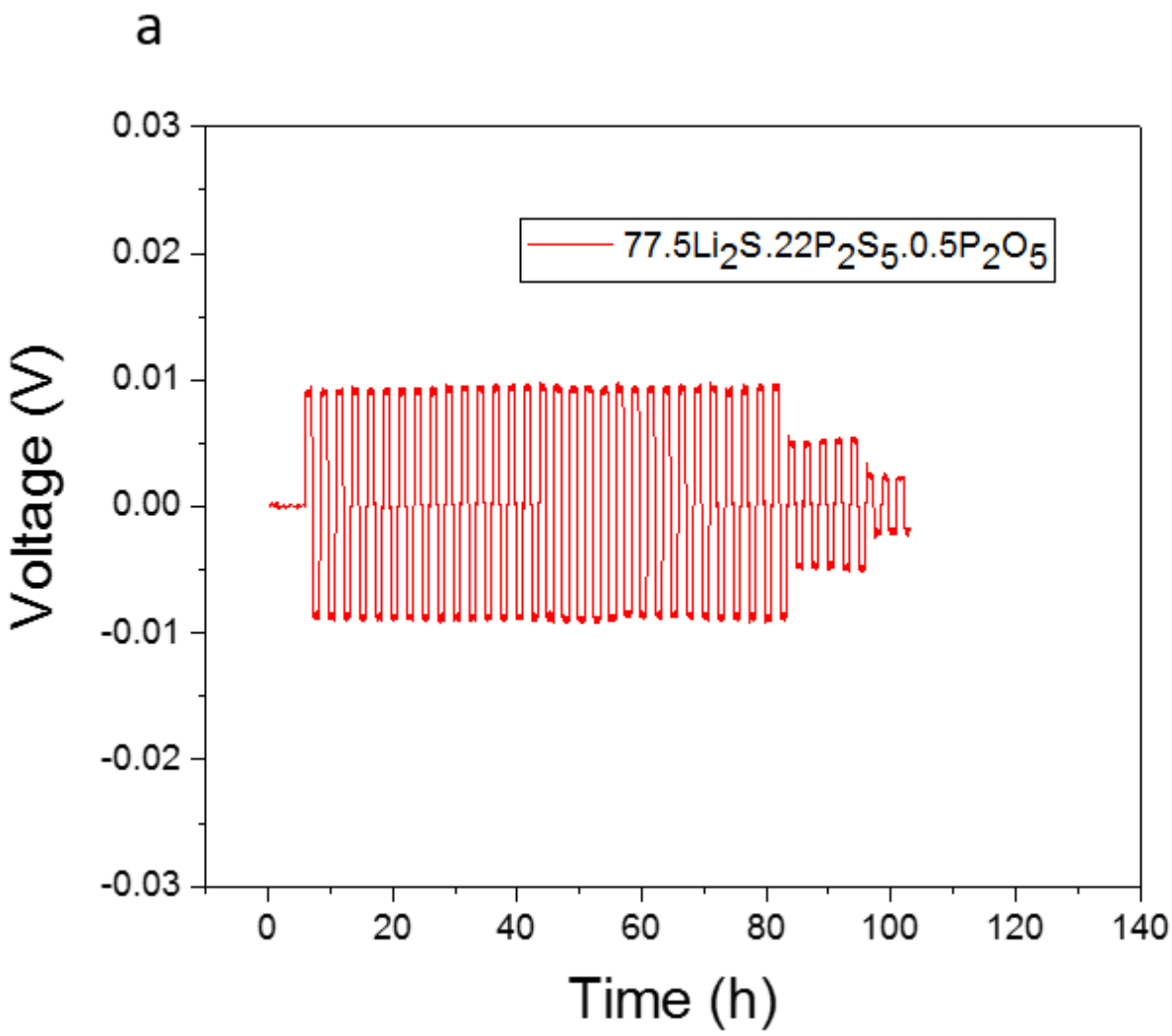
a
0.03
0.02
0.01
0.00
-0.01
-0.02
-0.03
Voltage (V)
77.5Li2S.22P2S5.0.5P2O5
0
20
40
60
80
100
120
140
Time (h)

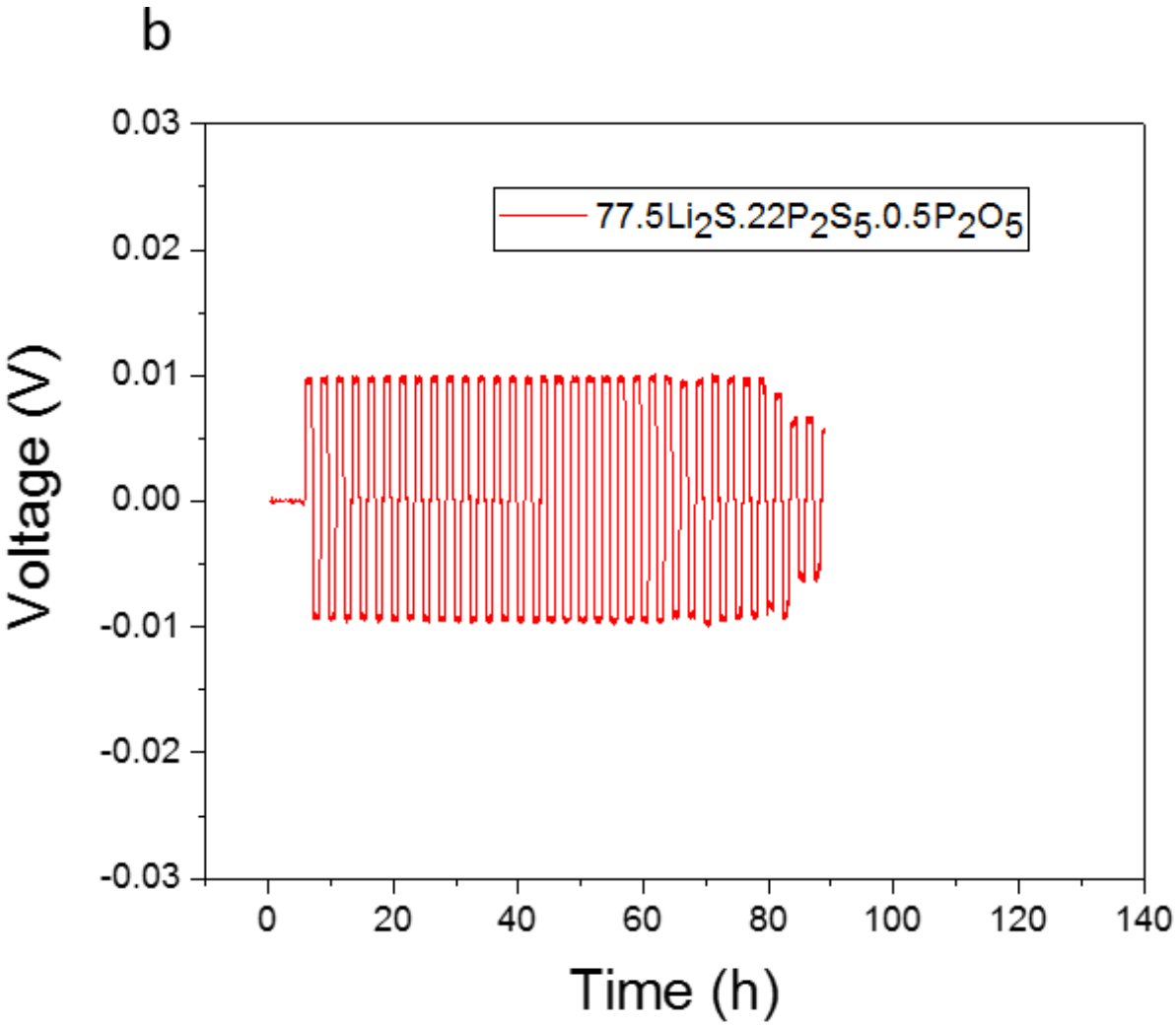

Figure 9. a) and b) show the cycling performance of the Li/77.5Li_2S.22P_2S_5.0.5P_2O_5 (mol %)/Li metal cells.

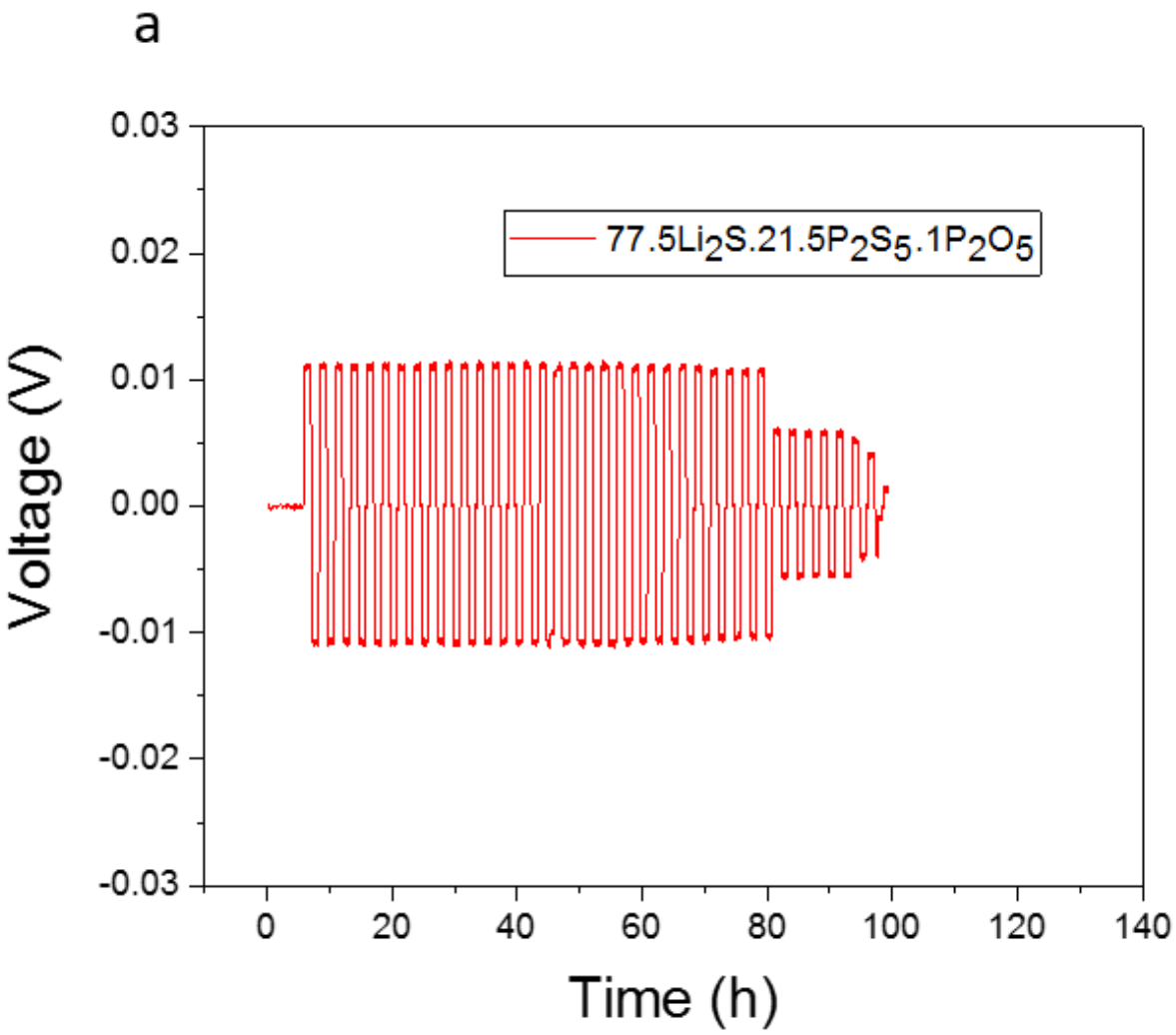
a
0.03
0.02
0.01
0.00
-0.01
-0.02
-0.03
Voltage (V)
77.5Li2S.21.5P2S5.1P2O5
0
20
40
60
80
100
120
140
Time (h)

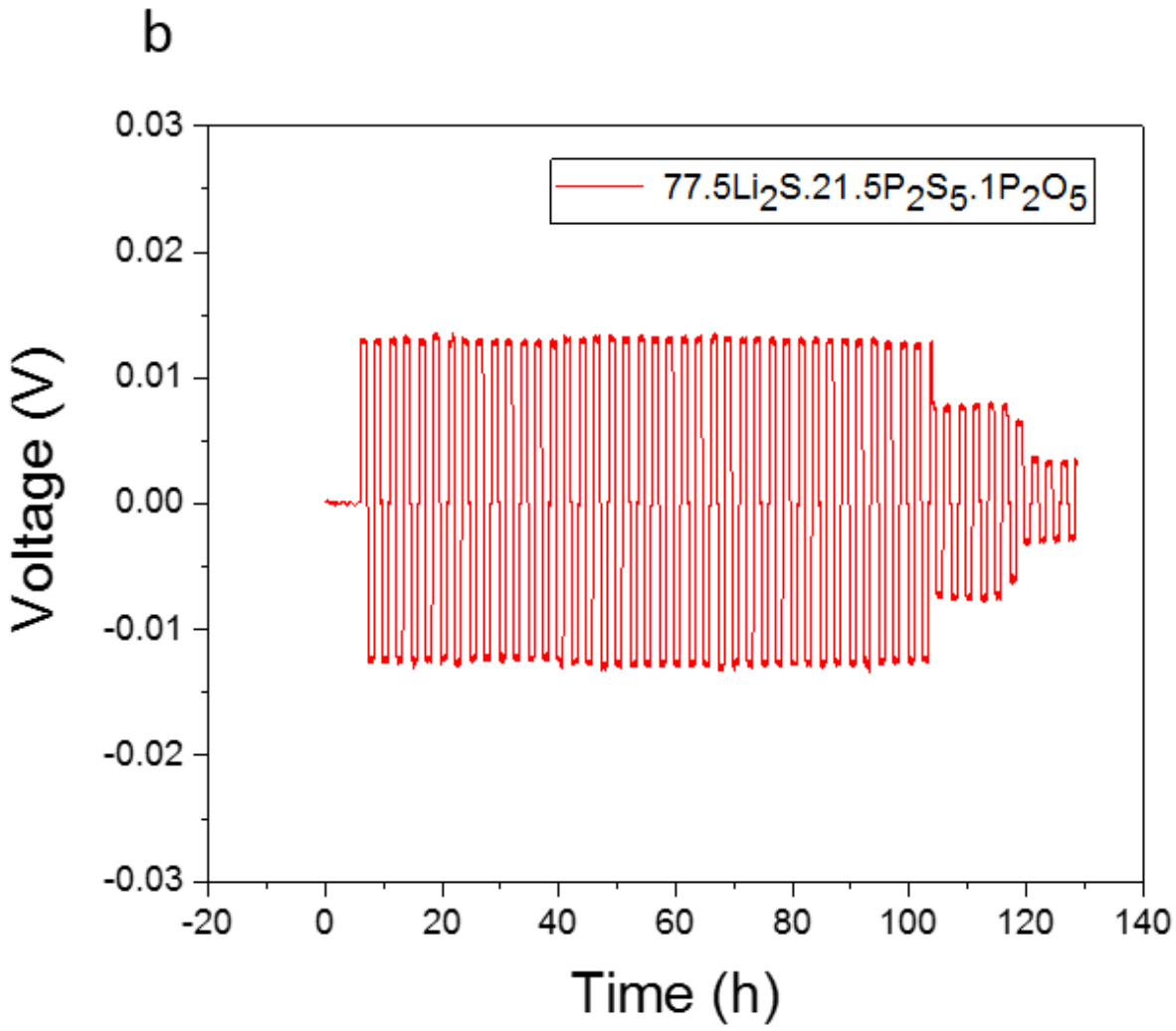

Figure 10. a) and b) show the cycling performance of the Li/77.5Li_2S.21.5P_2S_5.1P_2O_5 (mol %)/Li metal cells.

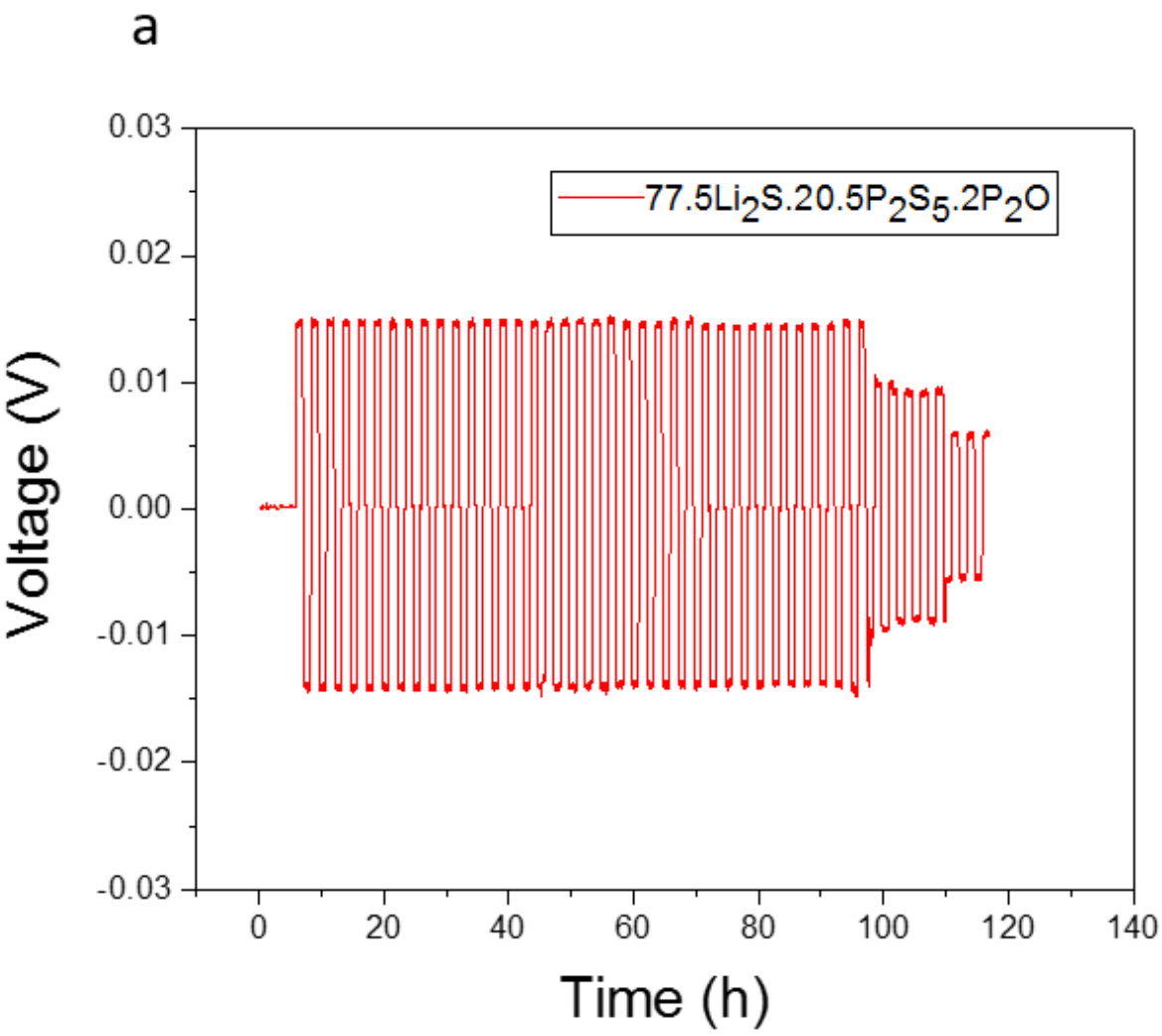
a
77.5Li2S.20.5P2S5.2P2O
Voltage (V)
0.03
0.02
0.01
0.00
-0.01
-0.02
-0.03
0
20
40
60
80
100
120
140
Time (h)

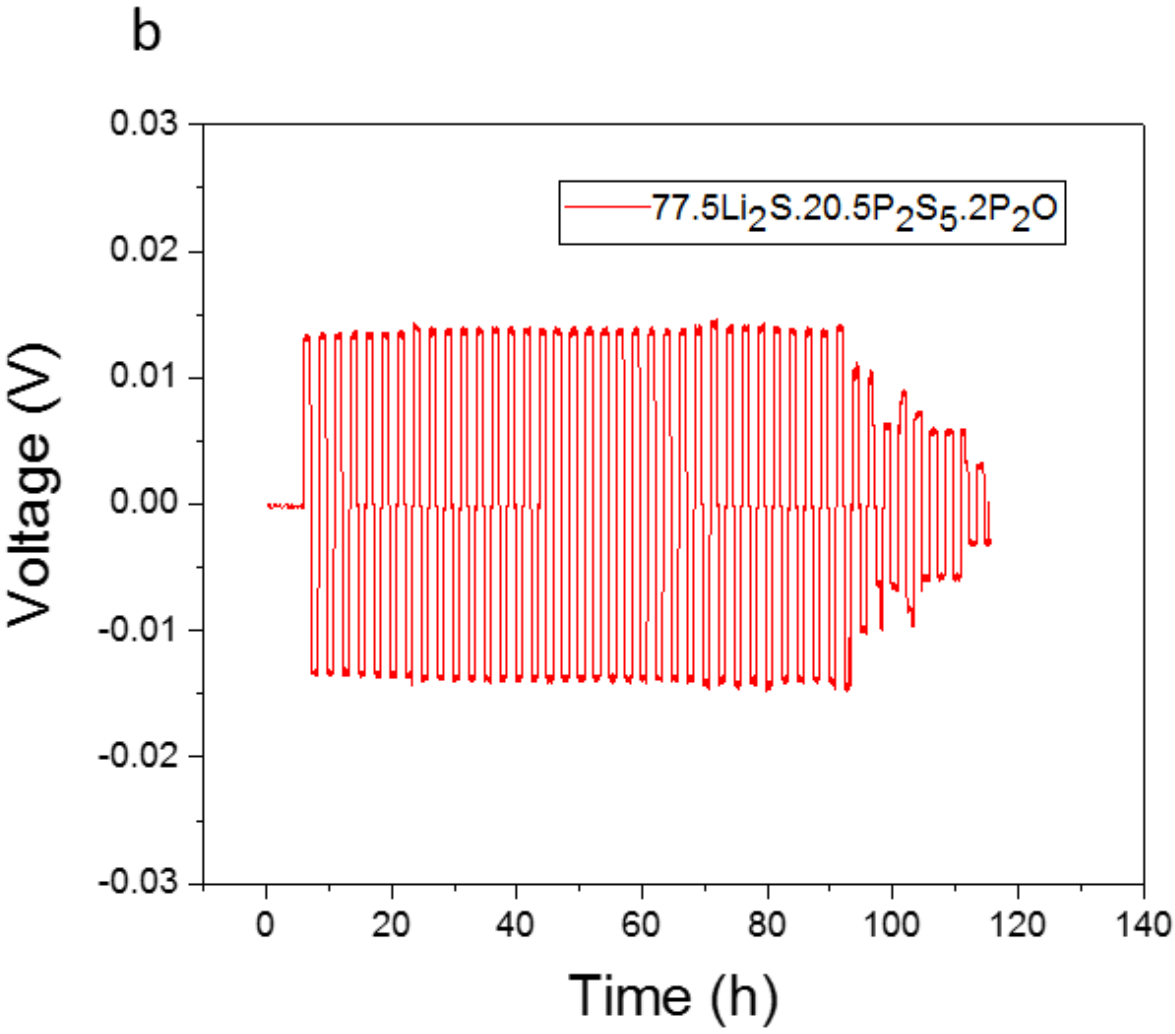

Figure 11. a) and b) show the cycling performance of Li/77.5Li_2S.20.5P_2S_5.2P_2O_5 (mol %)/Li metal cells.

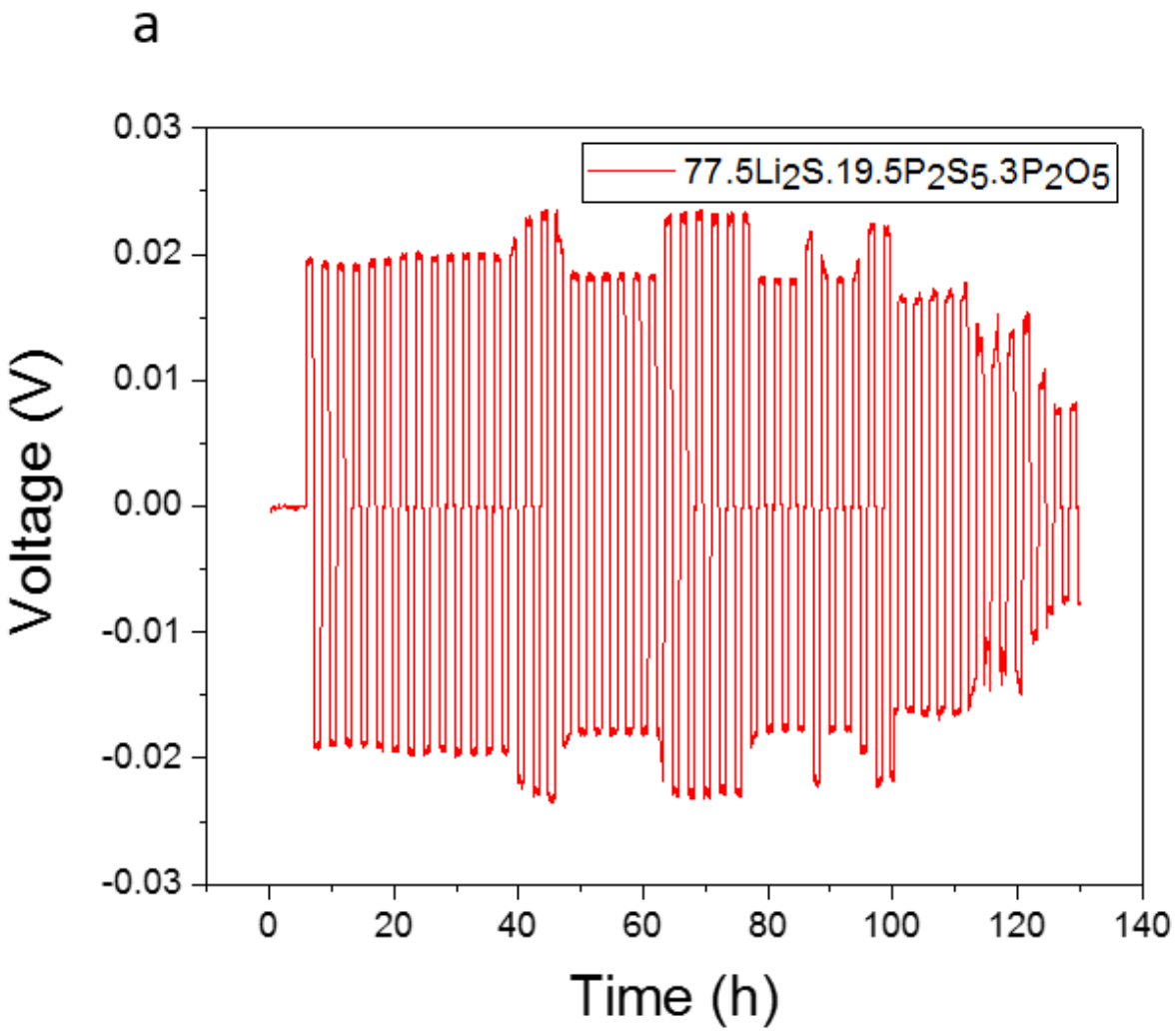
a
77.5Li2S.19.5P2S5.3P2O5
Voltage (V)
0.03
0.02
0.01
0.00
-0.01
-0.02
-0.03
0
20
40
60
80
100
120
140
Time (h)

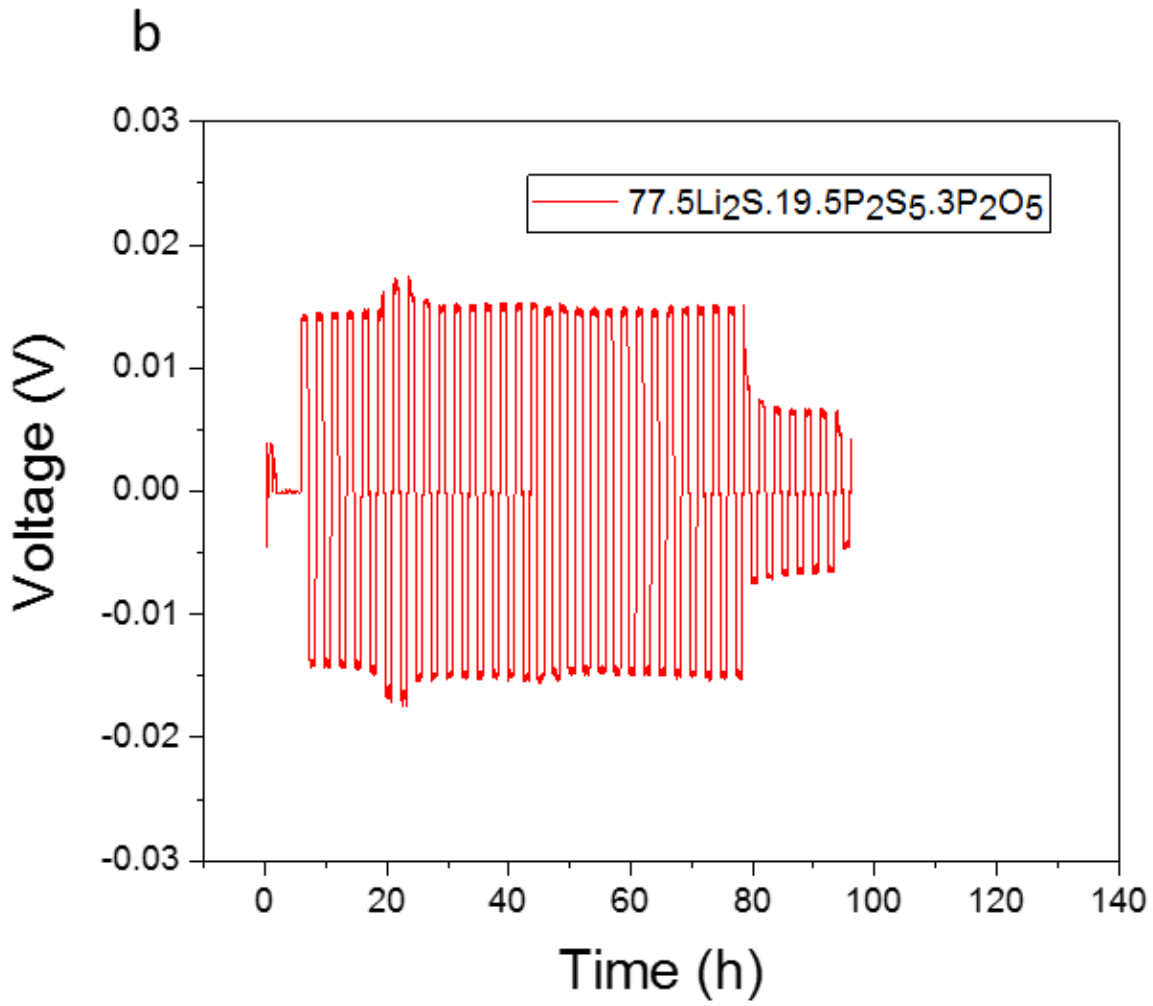

Figure 12. a) and b) show the cycling performance of the Li/77.5Li_2S.19.5P_2S_5.3P_2O_5 (mol %)/Li cells.

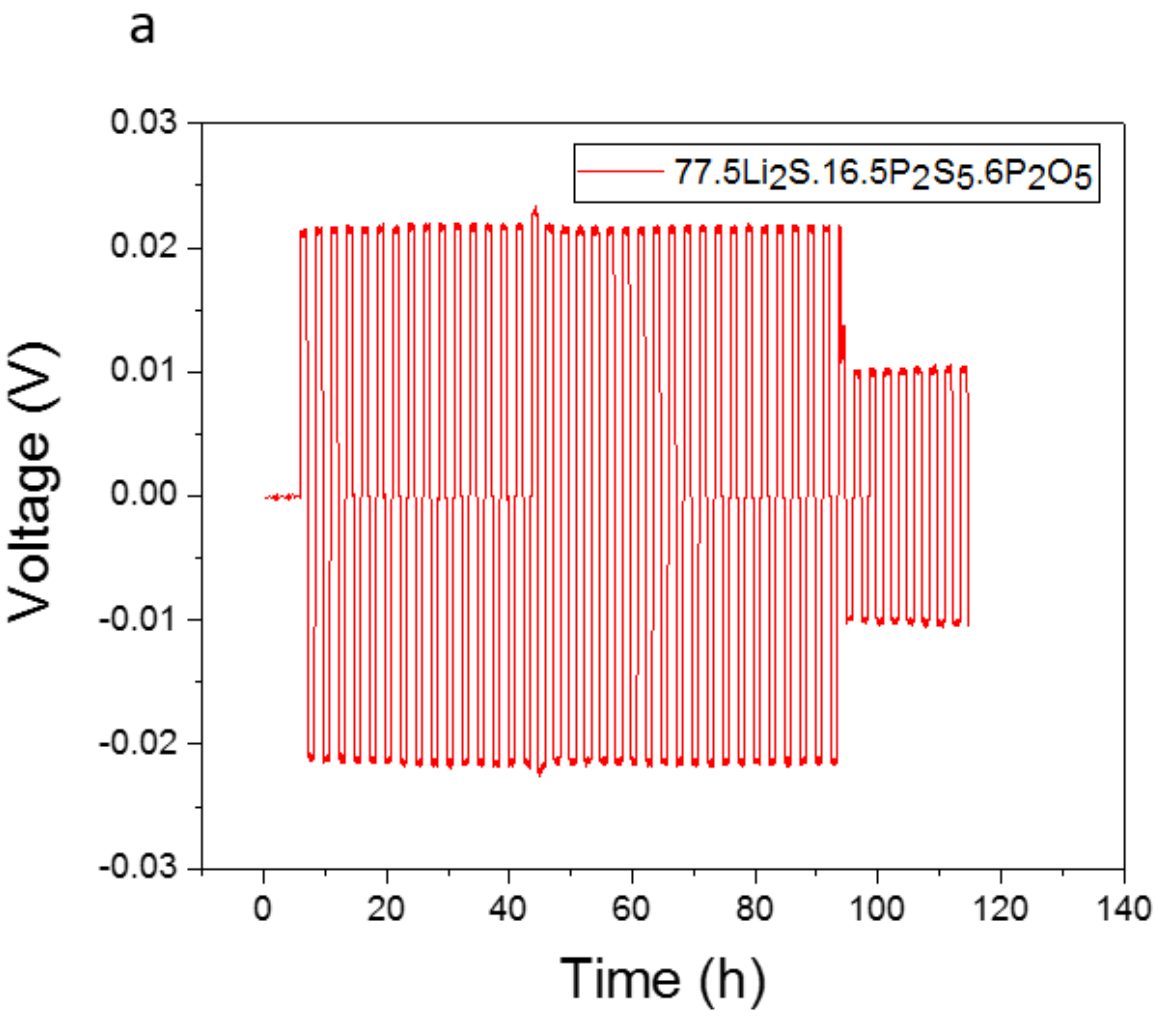
a
77.5Li2S.16.5P2S5.6P2O5
Voltage (V)
0.03
0.02
0.01
0.00
-0.01
-0.02
-0.03
0
20
40
60
80
100
120
140
Time (h)

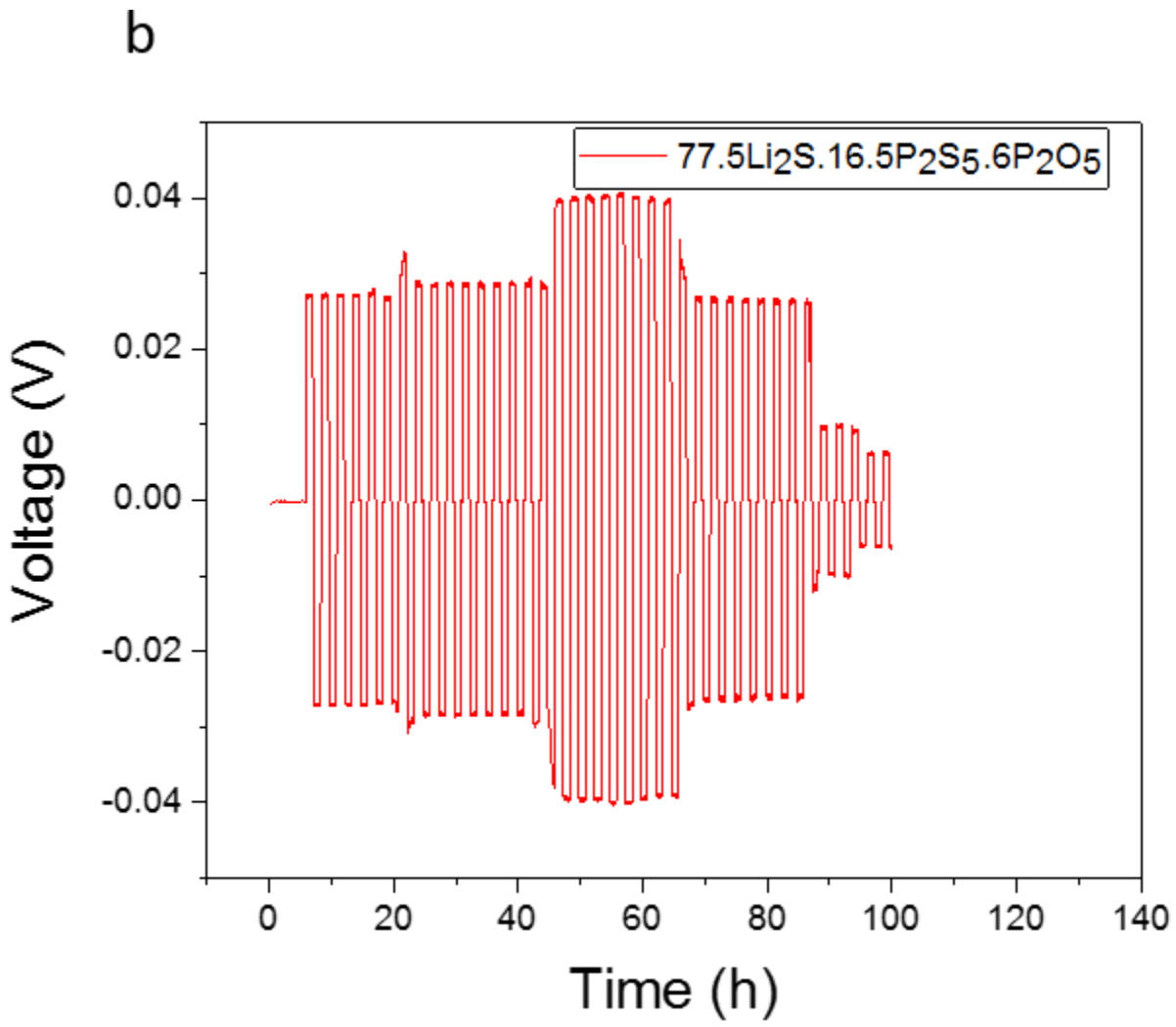

Figure 13. a) and b) show the cycling performance of the Li/77.5Li_2S.16.5P_2S_5.6P_2O_5 (mol %)/Li metal cells.

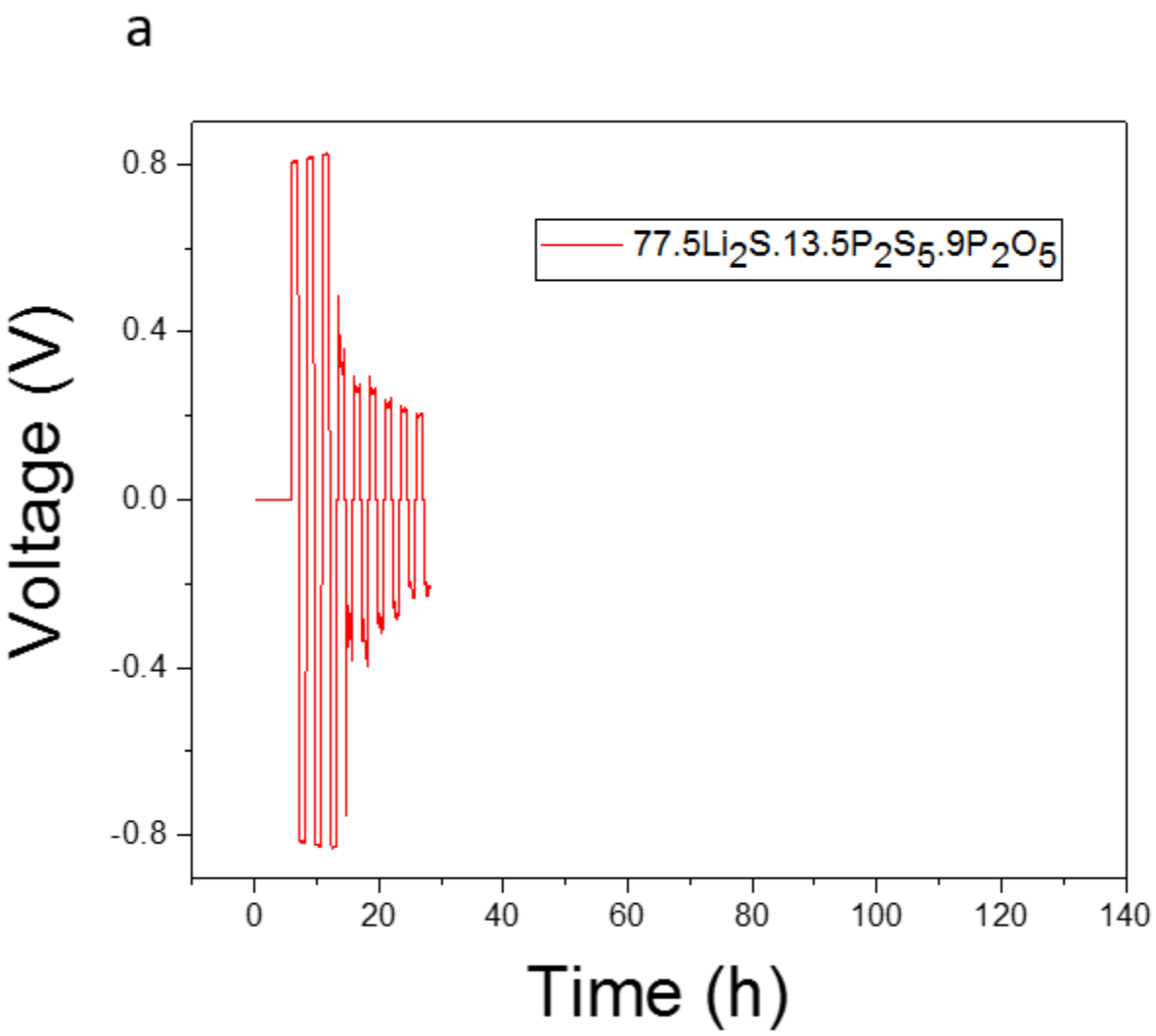
a
0.8
0.4
0.0
-0.4
-0.8
Voltage (V)
77.5Li2S.13.5P2S5.9P2O5
0
20
40
60
80
100
120
140
Time (h)

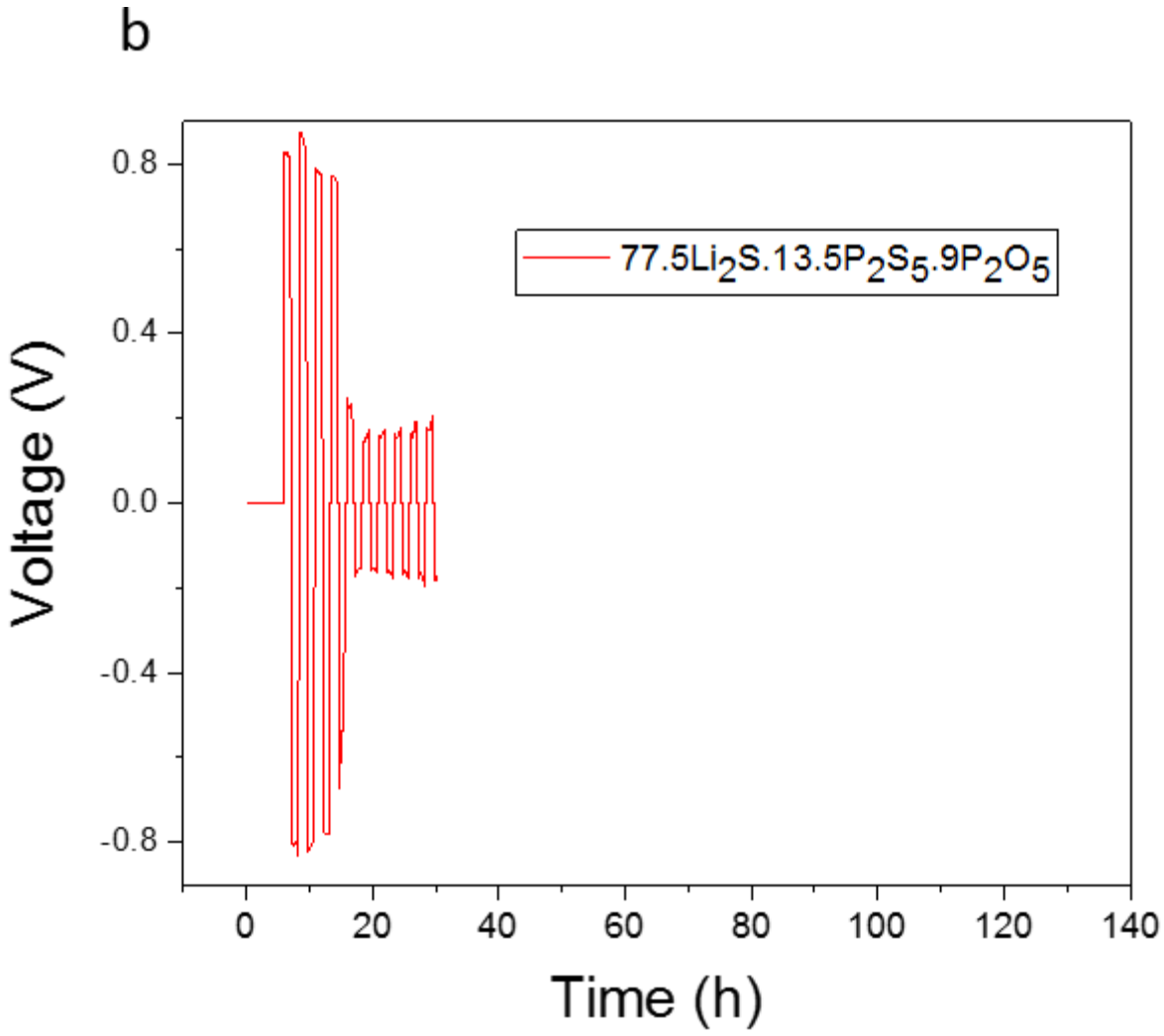

Figure 14. a) and b) show the cycling performance of the Li/77.5Li_2S.13.5P_2S_5.9P_2O_5 (mol %)/Li metal cells.

Figure 15 is short circuit capacity as function of P_2O_5 substitutions at the fixed current of 0.1 mA/cm^2. Also, the results of the deposition tests with varies P_2O_5 compositions are shown in figure 16, 17, 18, 19, 20, 21, and 22 below. Two deposition tests of each P_2O_5 substitutions were demonstrated to support the accuracy of the figure 15. The $77.5Li_2S.(22.5 - x)P_2S_5.xP_2O_5$ (mol %) glassy SSE with 0.5 mol% P_2O_5 displayed the highest short circuit capacity of 4.5 mAh/cm^2. This could be from enhanced conductivity in the electrolyte and increased density of the pellet. Moreover, the short circuit capacity of Li/$77.5Li_2S.(22.5 - x)P_2S_2.xP_2O_5$(mol %)/Li metal cells with 0.25, 1,2 and 3 mol% P_2O_5 substitutions were similar to short circuit capacity of Li/$77.5Li_2S.22.5P_2S_5$(mol %)/Li cells. Additionally, 9 mol% P_2O_5 substitution had the lowest short circuit capacity of 0.2 mAh/cm^2. This could be from diminished conductivity in the electrolyte and decreased density of the pellet.

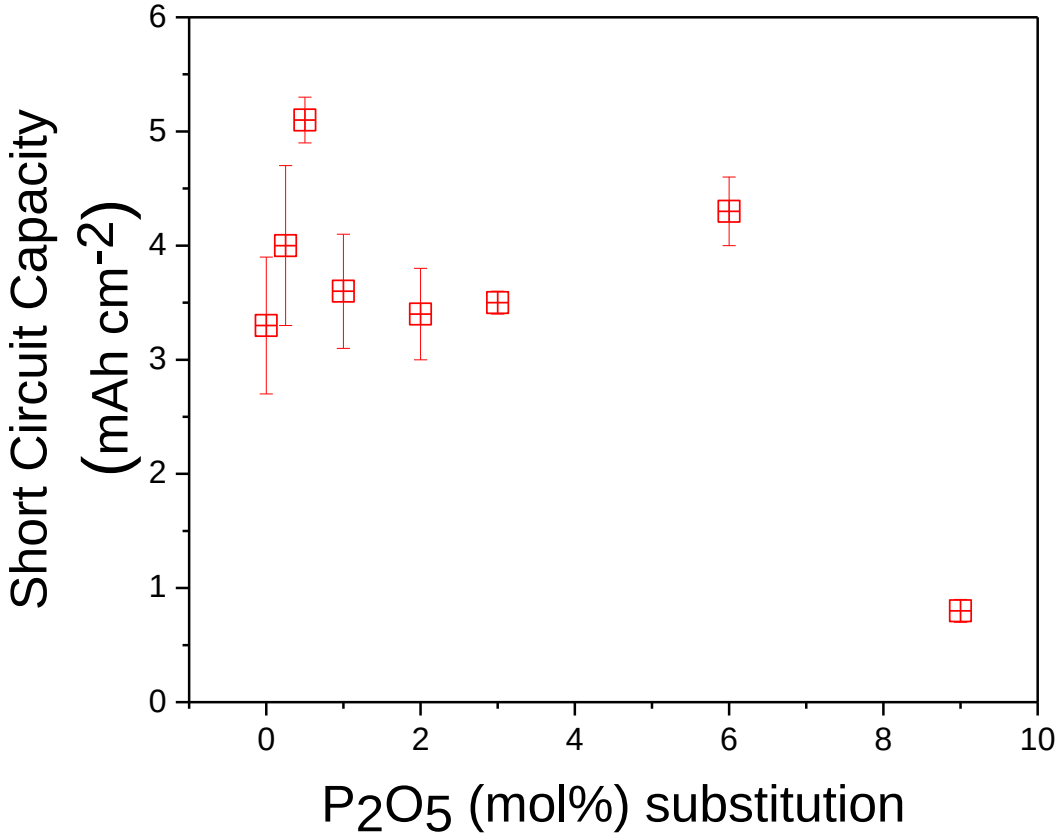

Figure 15. Shot circuit capacity of symmetric cell with using the $77.5Li_2S.(22.5 - x).P_2S_5.xP_2O_5$ (mol %) solid electrolyte at 0.1 mA/cm^2 with different variants of P_2O_5.

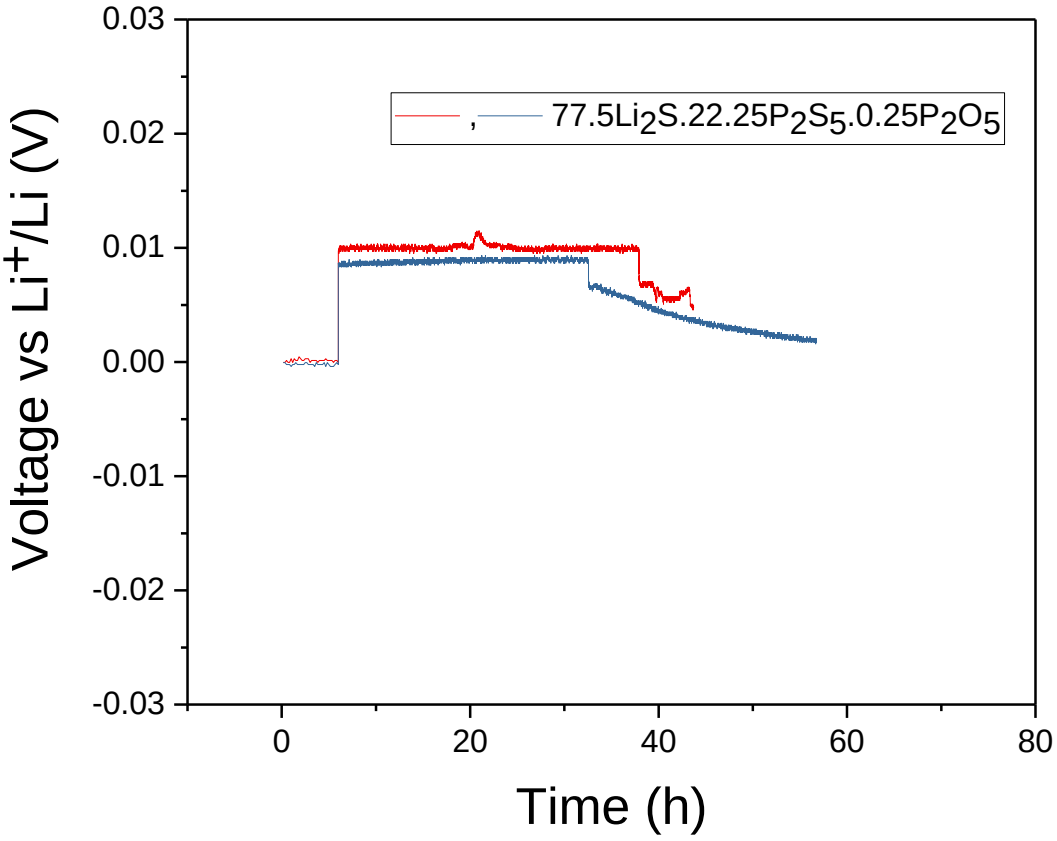

Figure 16. Galvanostatic plating of lithium in a metal cell using the $77.5Li_2S.(22.5 - x).P_2S_5.xP_2O_5$ (mol %) SSE with 0.25 mol% P_2O_5 substitution.

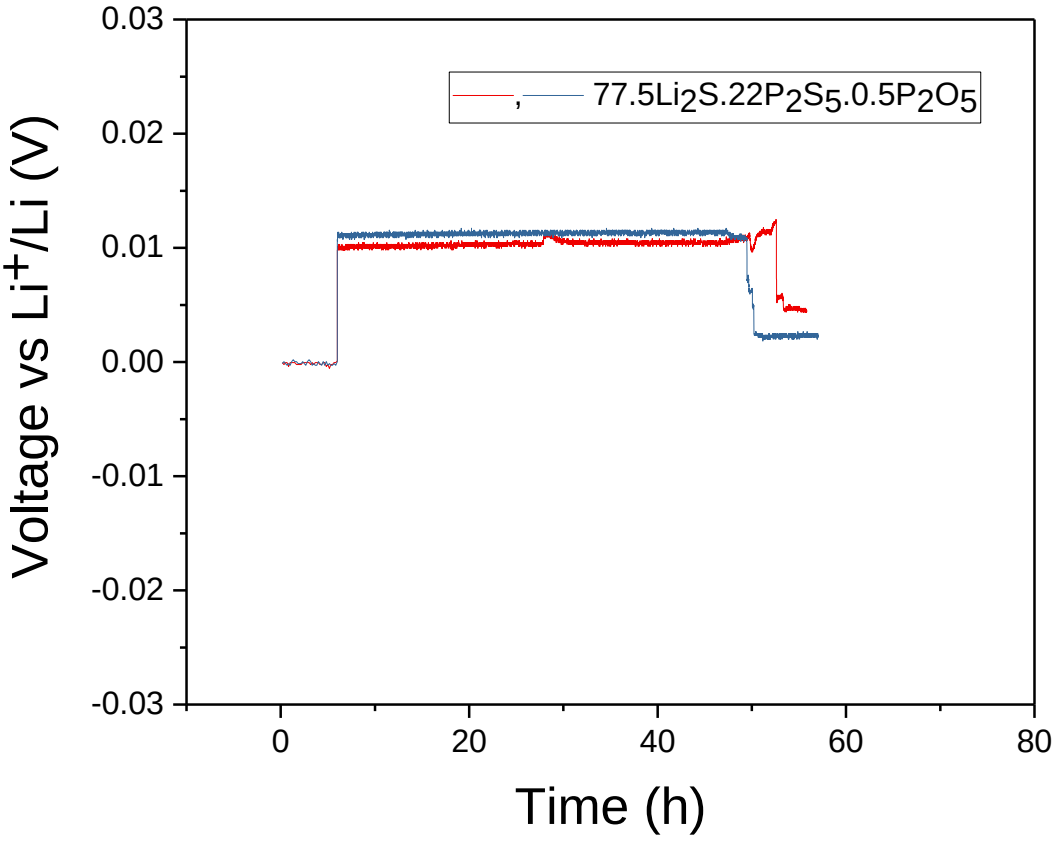

Figure 17. Galvanostatic plating of lithium in a metal cell using the $77.5Li_2S.(22.5 - x).P_2S_5.xP_2O_5$ (mol %) SSE with 0.5 mol% P_2O_5 substitution.

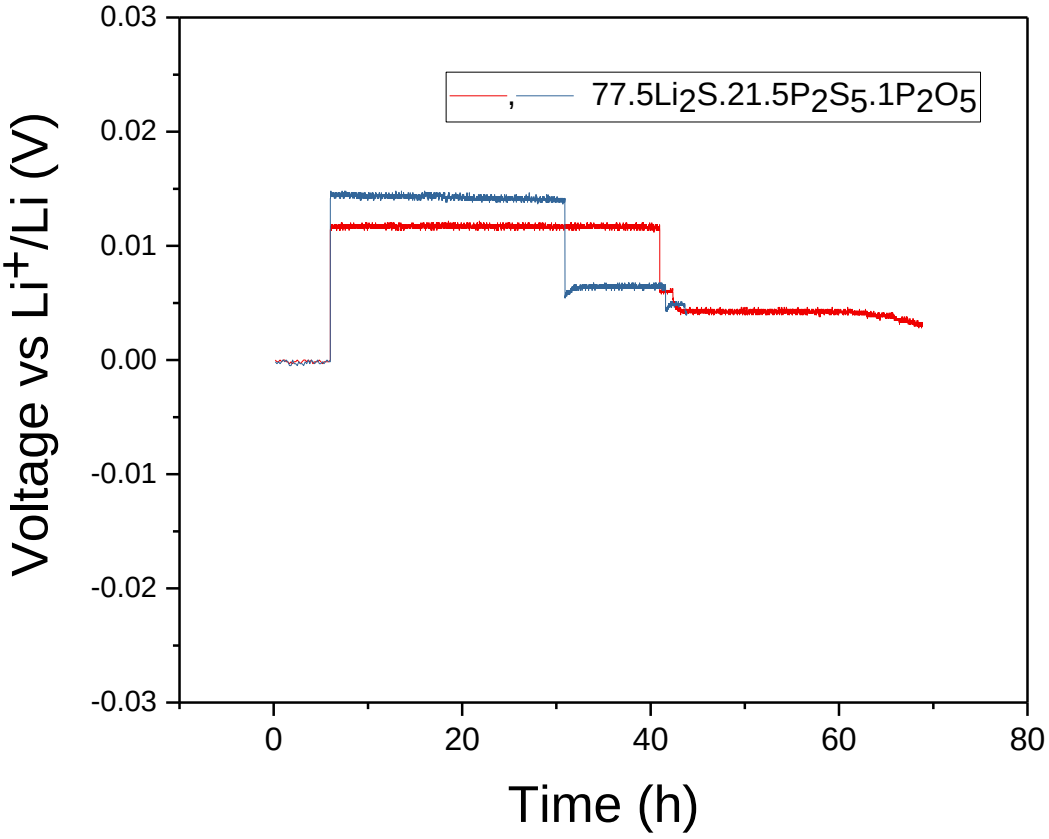

Figure 18. Galvanostatic plating of lithium in a metal cell the $77.5Li_2S.(22.5 - x).P_2S_5.xP_2O_5$ (mol %) SSE with 1 mol% P_2O_5 substitution.

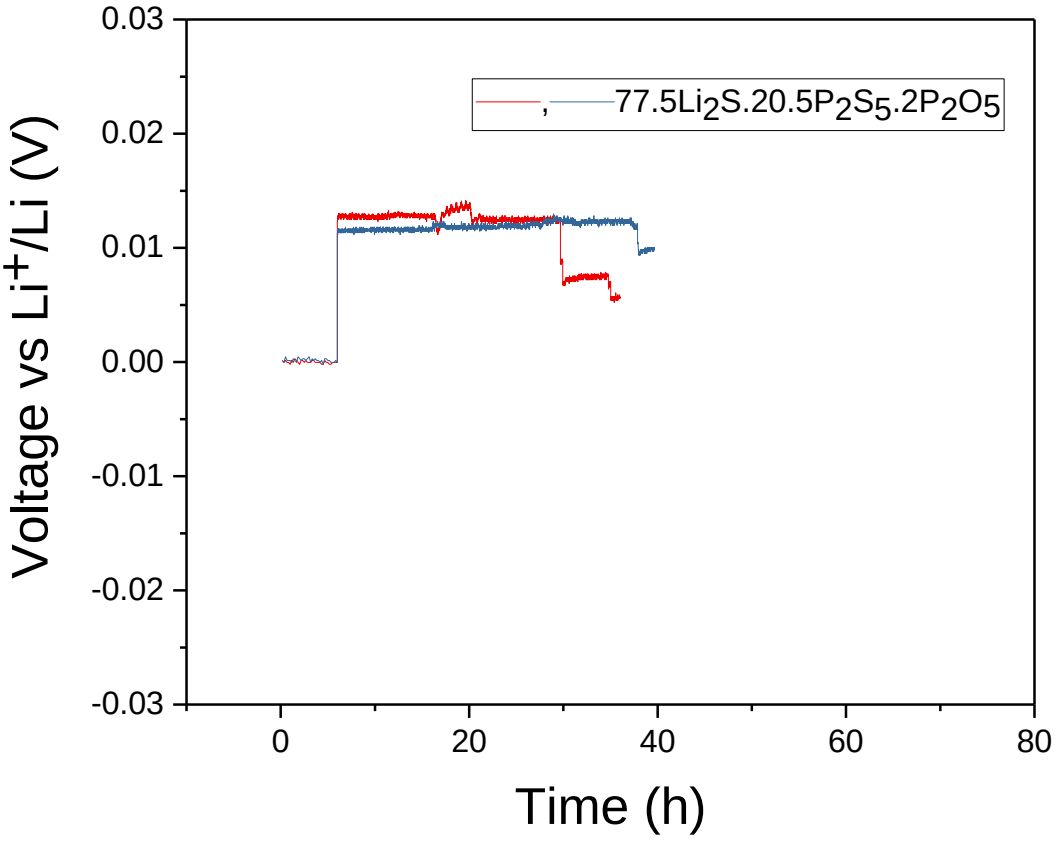

Figure 19. Galvanostatic plating of lithium in a metal cell using the $77.5Li_2S.(22.5 - x).P_2S_5.xP_2O_5$ (mol %) SSE with 2 mol% P_2O_5 substitution.

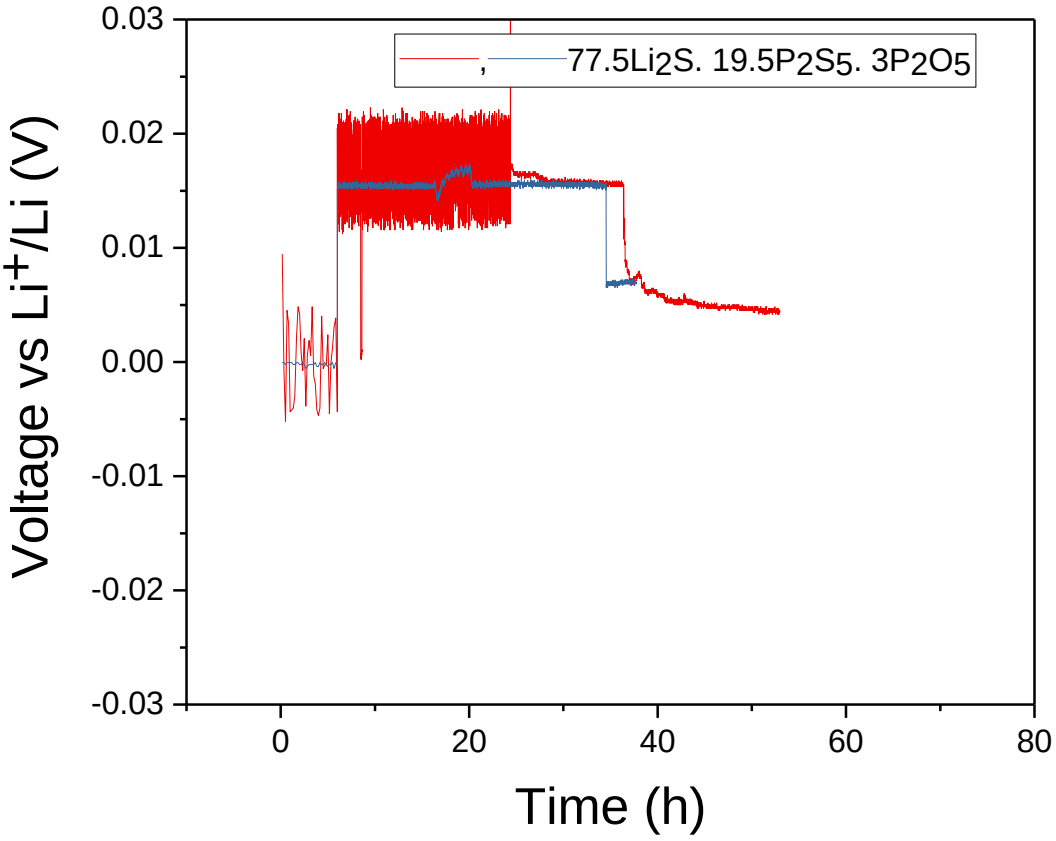

Figure 20. Galvanostatic plating of lithium in a metal cell using the $77.5Li_2S.(22.5 - x).P_2S_5.xP_2O_5$ (mol %) SSE with 3 mol% P_2O_5 substitution.

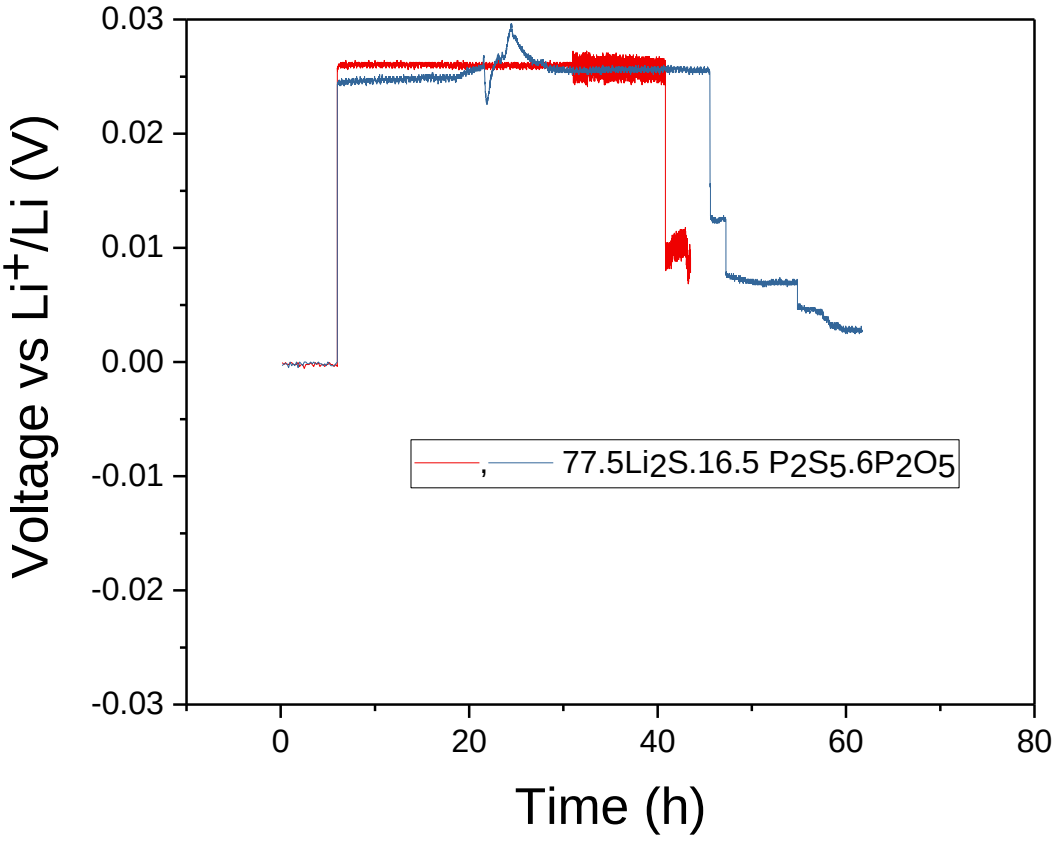

Figure 21. Galvanostatic plating of lithium in a metal cell using the $77.5Li_2S.(22.5 - x).P_2S_5.xP_2O_5$ (mol %) SSE with 6 mol% P_2O_5 substitution.

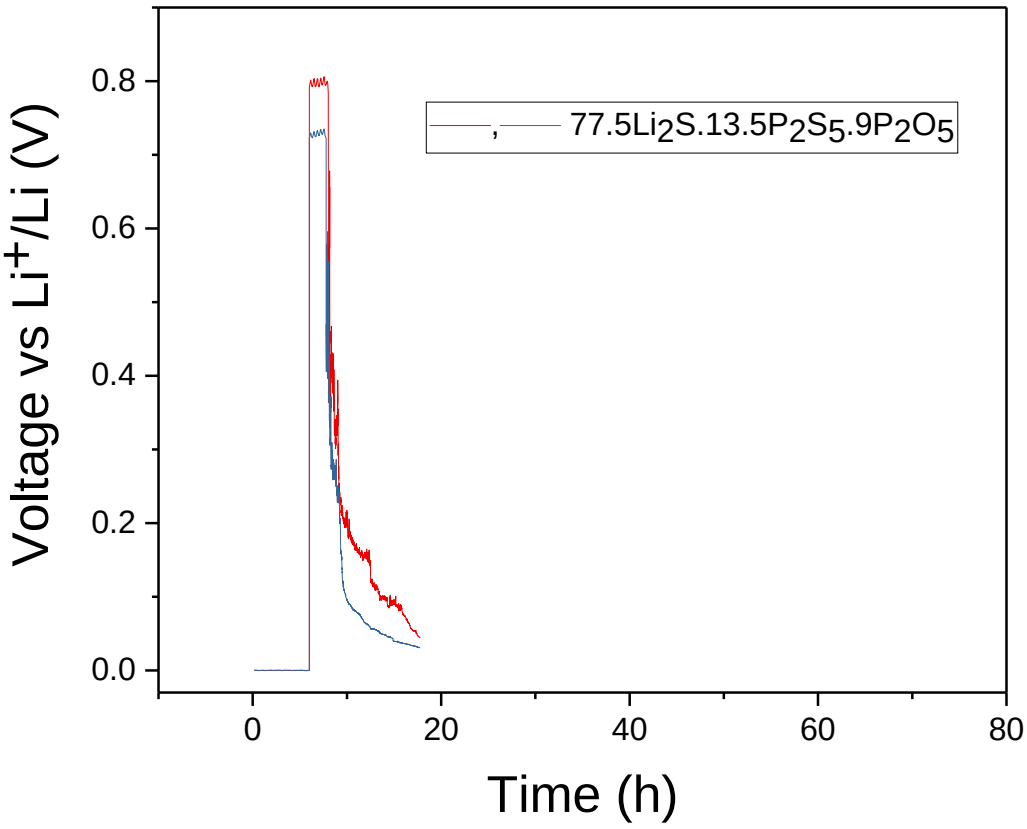

Figure 22. Galvanostatic plating of lithium in a metal cell using the $77.5Li_2S.(22.5\text{-}x).P_2S_5.xP_2O_5$ (mol %) SSe with 9 mol% P_2O_5 substitution.

4. Conclusions

The $77.5Li_2S.22.5P_2S_5$ glassy SSE and $77.5Li_2S.(22.5–x)P_2S_5.xP_2O_5$ (mol %) glassy electrolyte systems with varying composition of P_2O_5 were prepared by the mechanical milling method. Adding a small amount of P_2O_5 to $77.5Li_2S.22.5P_2S_5$ glassy electrolyte led to increase in conductivity, and density of the pellet. 0.25 mol % P_2O_5 substitution reveals the highest conductivity of 6.5×10^{-4} Scm^{-1} and the longest cycling performance of 54 cycles. This would be a result of the enhanced conductivity, and increased density of the pellet. Moreover, Li/$77.5Li_2S.(22.5–x).P_2S_5.xP_2O_5$ (mol %)/Li metal cells with P_2O_5 substitution of $x<9$ displayed longer cycling performance without short circuiting compared to cells with pure $77.5Li_2S.22.5P_2S_5$ (mol %) SSE. The increase of the cycling performances could be from enriched conductivity and P_2O_5 substitution. Furthermore, the $77.5Li_2S.(22.5–x)P_2S_5$ $.xP_2O_5$ (mol %) glassy electrolyte with 0.5 mol% P_2O_5 displayed the highest short circuit capacity. This could be from enhanced conductivity, and increased density of the pellet. Hence, in the case of this study, the conductivity, density and a small amount of P_2O_5 addition to the $77.5Li2S.22.5P_2S_5$ electrolyte could be the main concepts of diminished uncontrolled dendritic and moss lithium growth.

Bibliography

[1] Kamaya, N., Homma, K., Yamakawa, Y., Hirayama, M., Kanno, R., Yonemura, M., Kamiyama, T., Kato, Y., Hama, S., Kawamoto, K., and Mitsui, A., 2011, "A Lithium SuperionicConductor," Nat. Mater., **10**(9), pp. 682–686.

[2] Tarascon, J. M., and Armand, M., 2001, "Issues and Challenges Facing Rechargeable Lithium Batteries.," Nature, **414**(6861), pp. 359–367.

[3] Trevey, J. E., Gilsdorf, J. R., Miller, S. W., and Lee, S. H., 2012, "Li2S-Li2O-P2S5 solid Electrolyte for All-Solid-State Lithium Batteries," Solid State Ionics, **214**, pp. 25–30.

[4] Goodenough, J. B., and Kim, Y., 2010, "Challenges for Rechargeable Li Batteries," Chem. Mater., **22**(3), pp. 587–603.

[5] Inada, T., Takada, K., Kajiyama, A., Kouguchi, M., Sasaki, H., Kondo, S., Watanabe, M., Murayama, M., and Kanno, R., 2003, "Fabrications and Properties of Composite Solid-State Electrolytes," Solid State Ionics, **158**(3–4), pp. 275–280.

[6] Knauth, P., 2009, "Inorganic Solid Li Ion Conductors: An Overview," Solid State Ionics, **180**(14–16), pp. 911–916.

[7] Kim, J. G., Son, B., Mukherjee, S., Schuppert, N., Bates, A., Kwon, O., Choi, M. J., Chung, H. Y., and Park, S., 2015, "A Review of Lithium and Non-Lithium Based Solid State Batteries," J. Power Sources, **282**, pp. 299–322.

[8] Judez, X., Zhang, H., Li, C., Eshetu, G. G., González-Marcos, J. A., Armand, M., and Rodriguez-Martinez, L. M., 2018, "Review—Solid Electrolytes for Safe and High Energy Density Lithium-Sulfur Batteries: Promises and Challenges," J. Electrochem. Soc., **165**(1), pp. A6008–A6016.

[9] Kerman, K., Luntz, A., Viswanathan, V., Chiang, Y.-M., and Chen, Z., 2017, "Review—Practical Challenges Hindering the Development of Solid State Li Ion Batteries," J. Electrochem.Soc., **164**(7), pp. A1731–A1744.

[10] Bachman, J. C., Muy, S., Grimaud, A., Chang, H.-H., Pour, N., Lux, S. F., Paschos, O., Maglia, F., Lupart, S., Lamp, P., Giordano, L., and Shao-Horn, Y., 2016, "Inorganic Solid-State Electrolytes for Lithium Batteries: Mechanisms and Properties Governing Ion Conduction," Chem. Rev., **116**(1), pp. 140–162.

[11] Manthiram, A., Yu, X., and Wang, S., 2017, "Lithium Battery Chemistries Enabled by Solid-State Electrolytes," Nat. Rev. Mater., **2**(4), pp. 1–16.

[12] Sun, C., Liu, J., Gong, Y., Wilkinson, D. P., and Zhang, J., 2017, "Recent Advances in All-Solid-State Rechargeable Lithium Batteries," Nano Energy, **33**(January), pp. 363–386.

[13] Kerman, K., and Ramanathan, S., 2014, "Complex Oxide Nanomembranes for Energy Conversion and Storage: A Review," J. Mater. Res., **29**(3), pp. 320–337.

[14] Takeuchi, T., Kageyama, H., Nakanishi, K., Ohta, T., Sakuda, A., Sakaebe, H., Kobayashi, H.,Tatsumi, K., and Ogumi, Z., 2014, "10,Rapid Preparation of Li2S-P2S5 Solid Electrolyte and Its Application for Graphite/Li2S All-Solid-State Lithium Secondary Battery," ECS Electrochem. Lett., **3**(5), pp. A31–A35.

[15] Seino, Y., Takada, K., Kim, B. C., Zhang, L., Ohta, N., Wada, H., Osada, M., and Sasaki, T., 2005, "Synthesis of Phosphorous Sulfide Solid Electrolyte and All-Solid-State Lithium Batteries with Graphite Electrode," Solid State Ionics, **176**(31–34), pp. 2389–2393.

[16] Sakuda, A., Hayashi, A., and Tatsumisago, M., 2013, "Sulfide Solid Electrolyte with

Favorable Mechanical Property for All-Solid-State," pp. 2–6.

[17] Nagao, M., Hayashi, A., and Tatsumisago, M., 2011, "Sulfur-Carbon Composite Electrode for All-Solid-State Li/S Battery with Li 2S-P 2S 5 Solid Electrolyte," Electrochim. Acta, **56**(17), pp. 6055–6059.

[18] Mauger, A., Armand, M., Julien, C. M., and Zaghib, K., 2017, "Challenges and Issues Facing Lithium Metal for Solid-State Rechargeable Batteries," J. Power Sources, **353**, pp. 333–342.

[19] Kato, Y., Hori, S., Saito, T., Suzuki, K., Hirayama, M., Mitsui, A., Yonemura, M., Iba, H., and Kanno, R., 2016, "High-Power All-Solid-State Batteries Using Sulfide Superionic Conductors," Nat. Energy, **1**(4), p. 16030.

[20] Ceder, G., 2015, "A Solid Future," pp. 6–7.

[21] Chen, S., Xie, D., Liu, G., Mwizerwa, J. P., Zhang, Q., Zhao, Y., Xu, X., and Yao, X., 2018, "Sulfide Solid Electrolytes for All-Solid-State Lithium Batteries: Structure, Conductivity, Stability and Application," Energy Storage Mater., **14**(December 2017), pp. 58–74.

[22] Xu, R., Zhang, S., Wang, X., Xia, Y., Xia, X., Wu, J., Gu, C., and Tu, J., 2018, "Recent Developments of All-Solid-State Lithium Secondary Batteries with Sulfide Inorganic Electrolytes," Chem. - A Eur. J., pp. 1–13.

[23] Whiteley, J. M., Taynton, P., Zhang, W., and Lee, S. H., 2015, "Ultra-Thin Solid-State Li-Ion Electrolyte Membrane Facilitated by a Self-Healing Polymer Matrix," Adv. Mater., **27**(43), pp. 6922–6927.

[24] Yersak, T. A., Macpherson, H. A., Kim, S. C., Le, V. D., Kang, C. S., Son, S. B., Kim, Y. H., Trevey, J. E., Oh, K. H., Stol dt, C., and Lee, S. H., 2013, "Solid State Enabled Reversible Four Electron Storage," Adv. Energy Mater., **3**(1), pp. 120–127.

[25] Janek, J., and Zeier, W. G., 2016, "A Solid Future for Battery Development," Nat. Energy, **1**(9), pp. 1–4.

[26] Whiteley, J. M., Hafner, S., Zhu, C., Zhang, W., and Lee, S.-H., 2017, "Stable Lithium Deposition Using a Self-Optimizing Solid Electrolyte Composite," J. Electrochem. Soc., **164**(13), pp. A2962–A2966.

[27] Raj, R., and Wolfenstine, J., 2017, "Current Limit Diagrams for Dendrite Formation in Solid-State Electrolytes for Li-Ion Batteries," J. Power Sources, **343**, pp. 119–126.

[28] Sudo, R., Nakata, Y., Ishiguro, K., Matsui, M., Hirano, A., Takeda, Y., Yamamoto, O., and Imanishi, N., 2014, "Interface Behavior between Garnet-Type Lithium-Conducting Solid Electrolyte and Lithium Metal," Solid State Ionics, **262**, pp. 151–154.

[29] Lotsch, B. V., and Maier, J., 2017, "Relevance of Solid Electrolytes for Lithium-Based Batteries: A Realistic View," J. Electroceramics, **38**(2–4), pp. 128–141.

[30] Aguesse, F., Manalastas, W., Buannic, L., Del Amo, J. M. L., Singh, G., Llordés, A., and Kilner, J., 2017, "Investigating the Dendritic Growth during Full Cell Cycling of Garnet Electrolyte in Direct Contact with Li Metal," ACS Appl. Mater. Interfaces, **9**(4), pp. 3808–3816.

[31] Sharafi, A., Meyer, H. M., Nanda, J., Wolfenstine, J., and Sakamoto, J., 2016, "Characterizing the Li-Li7La3Zr2O12interface Stability and Kinetics as a Function of Temperature and Current Density," J. Power Sources, **302**, pp. 135–139.

[32] Basappa, R. H., Ito, T., and Yamada, H., 2017, "Contact between Garnet-Type Solid Electrolyte and Lithium Metal Anode: Influence on Charge Transfer Resistance and Short Circuit Prevention," J. Electrochem. Soc., **164**(4), pp. A666–A671.

[33] Bron, P., Roling, B., and Dehnen, S., 2017, "Impedance Characterization Reveals Mixed

Conducting Interphases between Sulfidic Superionic Conductors and Lithium Metal Electrodes," J. Power Sources, **352**, pp. 127–134.

[34] Tao, Y., Chen, S., Liu, D., Peng, G., Yao, X., and Xu, X., 2016, "Lithium Superionic Conducting Oxysulfide Solid Electrolyte with Excellent Stability against Lithium Metal for All-Solid-State Cells," J. Electrochem. Soc., **163**(2), pp. A96–A101.

[35] Porz, L., Swamy, T., Sheldon, B. W., Rettenwander, D., Frömling, T., Thaman, H. L., Berendts, S., Uecker, R., Carter, W. C., and Chiang, Y. M., 2017, "Mechanism of Lithium Metal Penetration through Inorganic Solid Electrolytes," Adv. Energy Mater., **7**(20), pp. 1–12.

[36] Minami, T., Hayashi, A., and Tatsumisago, M., 2000, "Preparation and Characterization of Lithium Ion-Conducting Oxysulfide Glasses," Solid State Ionics, **136**(137), pp. 1015–1023.

[37] Minami, K., Hayashi, A., and Tatsumisago, M., 2008, "Electrical and Electrochemical Properties of the 70Li2S·(30 - x)P2S5·xP2O5 Glass-Ceramic Electrolytes," Solid State Ionics, **179**(27–32), pp. 1282–1285.

[38] Minami, K., Mizuno, F., Hayashi, A., and Tatsumisago, M., 2008, "Structure and Properties of the 70Li2S · (30 - x)P2S5 · xP2O5 Oxysulfide Glasses and Glass-Ceramics," J. Non. Cryst. Solids, **354**(2–9), pp. 370–373.

[39] Minami, K., Hayashi, A., Ujiie, S., and Tatsumisago, M., 2011, "Electrical and Electrochemical Properties of Glass-Ceramic Electrolytes in the Systems Li2S-P2S5-P2S 3 and Li2S-P2S5-P2O5," Solid State Ionics, **192**(1), pp. 122–125.

[40] Ohtomo, T., Hayashi, A., Tatsumisago, M., and Kawamoto, K., 2013, "Characteristics of the Li2O-Li2S-P2S 5 Glasses Synthesized by the Two-Step Mechanical Milling," J. Non. Cryst. Solids, **364**(1), pp. 57–61.

[41] Mo, S., Lu, P., Ding, F., Xu, Z., Liu, J., Liu, X., and Xu, Q., 2016, "High-Temperature Performance of All-Solid-State Battery Assembled with 95(0.7Li2S-0.3P2S5)-5Li3PO4glass Electrolyte," Solid State Ionics, **296**, pp. 37–41.

[42] Huang, B., Yao, X., Huang, Z., Guan, Y., Jin, Y., and Xu, X., 2015, "Li3PO4-Doped Li7P3S11glass-Ceramic Electrolytes with Enhanced Lithium Ion Conductivities and Application in All-Solid-State Batteries," J. Power Sources, **284**, pp. 206–211.

[43] Kato, A., Nagao, M., Sakuda, A., Hayashi, A., and Tatsumisago M., 2014, "Evaluation of Young's Modulus of Li_2S-P_2S_5-P_2O_5 Oxysulfide Glass Solid Electrolytes," J. Ceram. Soc. Japan, **122**(1427), pp. 552–555.